nature ecology & evolution

Article

https://doi.org/10.1038/s41559-022-01923-8

Mutualism-enhancing mutations dominate early adaptation in a two-species microbial community

Received: 12 August 2021

Accepted: 3 October 2022

Published online: 2 January 2023

Check for updates

Sandeep Venkataram[1], Huan-Yu Kuo[1,2], Erik F. Y. Hom[3] & Sergey Kryazhimskiy[1]

Species interactions drive evolution while evolution shapes these interactions. The resulting eco-evolutionary dynamics and their repeatability depend on how adaptive mutations available to community members affect fitness and ecologically relevant traits. However, the diversity of adaptive mutations is not well characterized, and we do not know how this diversity is affected by the ecological milieu. Here we use barcode lineage tracking to address this question in a community of yeast *Saccharomyces cerevisiae* and alga *Chlamydomonas reinhardtii* that have a net commensal relationship that results from a balance between competitive and mutualistic interactions. We find that yeast has access to many adaptive mutations with diverse ecological consequences, in particular those that increase and reduce the yields of both species. The presence of the alga does not change which mutations are adaptive in yeast (that is, there is no fitness trade-off for yeast between growing alone or with alga), but rather shifts selection to favour yeast mutants that increase the yields of both species and make the mutualism stronger. Thus, in the presence of the alga, adaptative mutations contending for fixation in yeast are more likely to enhance the mutualism, even though cooperativity is not directly favoured by natural selection in our system. Our results demonstrate that ecological interactions not only alter the trajectory of evolution but also dictate its repeatability; in particular, weak mutualisms can repeatably evolve to become stronger.

Ecological communities are often perturbed by environmental shifts[1,2], demographic noise[3] and species turnover[4,5]. Such perturbations can not only displace communities from their ecological equilibria but also precipitate adaptive evolution[6–9]. Evolutionary changes within one species can be rapid and can alter its ecological interactions with other community members, which can cause further evolution[8–10]. Although such eco-evolutionary feedbacks appear to be widespread[7,9–25], the population genetic mechanisms that underlie them are not well understood[26]. For example, how does the spectrum of adaptive mutations available to a species (that is, the genomic locations of adaptive mutations and their fitness benefits) depend on the composition of the surrounding community? In particular, how does it change when a species is lost from the community or a new species invades it? How many and which of the adaptive mutations available to a species affect

[1]Department of Ecology, Behavior and Evolution, University of California San Diego, La Jolla, CA, USA. [2]Department of Physics, University of California San Diego, La Jolla, CA, USA. [3]Department of Biology and Center for Biodiversity and Conservation Research, University of Mississippi, University, MS, USA. e-mail: skryazhi@ucsd.edu

https://doi.org/10.1038/s41559-022-01923-8

its interactions with the rest of the community? Which of these mutations are likely to spread and fix? And thus, how diverse and repeatable are the ecological outcomes of evolution?

Empirical data supporting answers to these questions would help us develop a better theoretical understanding of eco-evolutionary dynamics. For example, many existing models assume that any combination of traits can be produced by mutations so that the eco-evolutionary trajectories are determined exclusively by natural selection[27]. However, recent evidence suggests that the availability of mutations can substantially impact evolution[28–32]. Yet, we know very little about the distributions of ecological and fitness effects of new mutations in multi-species communities and how these distributions shift when the ecological milieu changes—for example, owing to the addition or extinction of community members.

Here, we address this gap in one of the simplest experimentally tractable microbial communities. Our community consists of two species, the alga *Chlamydomonas reinhardtii* and the yeast *Saccharomyces cerevisiae*, that interact in our environment via competition and mutualism[33]. Although communities in nature often contain more members, understanding eco-evolutionary dynamics in simple model communities is helpful for developing an intuition and expectations for the behaviours of more complex ecosystems[34–36]. We measure how adaptive mutations arising in one member of our community, the yeast, affect its competitive fitness (a metric that determines the evolutionary success of a mutant lineage), the absolute abundances of both species in the community (a metric that informs us about the type of interactions between species and the stability of the community) as well as basic life-history traits of yeast (growth rates and carrying capacities) that contribute to both fitness and abundances. We specifically ask whether and how the statistical distribution of effects of adaptive mutations in yeast are altered by the presence/absence of the alga. To this end, we use the barcode lineage tracking (BLT) technology[37,38] to isolate hundreds of adaptive mutations arising in yeast when it evolves alone or in community with the alga. Our data offer us a detailed view on how inter-species interactions affect the evolutionary dynamics of new mutations, and how these mutations in turn alter the ecology of our community.

Results

Yeast and alga form a facultative competitive mutualism

In a previous study, Hom and Murray showed that, in a sealed environment in which nitrite is provided as a sole source of nitrogen and glucose is provided as a sole source of organic carbon, the yeast *S. cerevisiae* and the alga *C. reinhardtii* spontaneously form an obligate mutualism[33]. Under such conditions, *C. reinhardtii* consumes nitrite and produces ammonium that is secreted and utilized by *S. cerevisiae*, which consumes glucose and produces CO_2 that is in turn utilized by the alga. When the environment is opened to ambient gas exchange and ammonium is supplied in the medium, both the yeast and the alga can survive without each other, that is, the mutualism becomes facultative. In this study, we grow the yeast and the alga alone and together over multiple 5 day growth and dilution cycles in well-mixed and well-lit conditions, open to gas exchange, in a medium supplemented with 0.5 mM of ammonium (for details, see Methods).

Time-course cell-density measurements of the wild-type yeast and alga over a single cycle confirm that both species grow significantly differently in the community with each other than alone (Fig. 1 and Extended Data Fig. 1; repeated-measures analysis of variance (ANOVA) $P = 10^{-4}$ for the yeast and $P = 5 \times 10^{-8}$ for the alga), indicating that they ecologically interact in our experimental environment. Specifically, the alga achieves higher densities over the entire growth cycle in the community than alone. It thus clearly benefits from its interaction with yeast. Meanwhile, yeast reaches lower peak density at 48 h in the presence of the alga than alone (Fig. 1a), which indicates that it initially suffers from competition against the alga, probably for

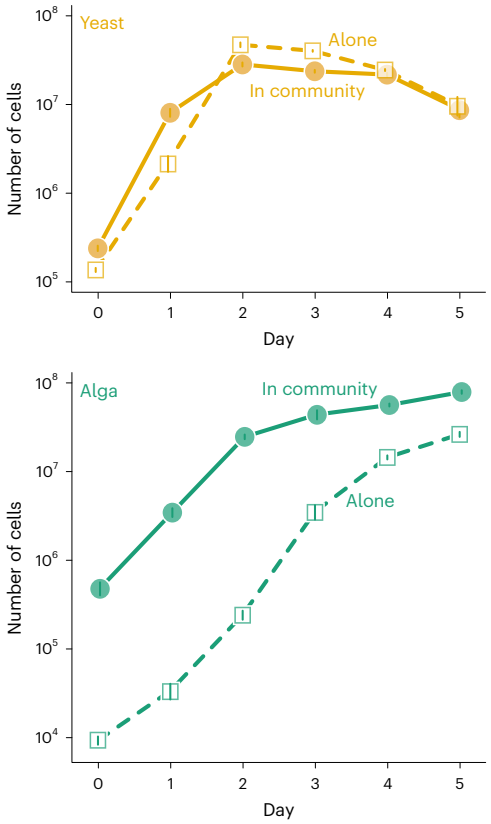

Fig. 1 | Growth of ancestral yeast and alga. Growth of the ancestral yeast and alga alone (solid lines) and in a community (dashed lines) over the 5-day cycle. Error bars show ±1 standard error of the mean (s.e.m.) ($n = 6$ except yeast alone where $n = 4$).

ammonium. Upon the depletion of supplemented ammonium, the alga subsequently reduces nitrite to ammonium that it then secretes[33]. This nitrogen provisioning by the alga reduces the yeast's rate of population decline between days 3 and 4 (t-test $P = 5 \times 10^{-4}$; Extended Data Fig. 1 and Supplementary Table 1). The result of this benefit is that yeast reaches approximately the same density by the end of the cycle in the community as it does alone, despite having a lower peak density on day 2. As yeast and alga initially compete and later cooperate in our conditions, we refer to our system as a competitive mutualism[39].

To summarize the net effects of these complex ecological interactions, we compare the yields (that is, cell densities at the end of the 5-day cycle) that both species achieve when growing in community versus alone (Fig. 1). Specifically, we compute the ratio of yeast yield in community (YYC) to its yield alone (YYA) and the ratio of alga yield in community (AYC) to its yield alone (AYA). Both ratios exceeding unity indicates that cooperation is overall more important than competition. Conversely, when both ratios are less than 1, competition is overall more important than cooperation. For our wild-type community, we find that the YYC-to-YYA ratio is not significantly different from 1, while the AYC-to-AYA ratio equals 3.00 (95% confidence interval (CI) 2.64–3.36, Student's t-test $t = 13.24$, df = 7.12, $P = 3 \times 10^{-6}$; Fig. 1). This indicates that the alga gains a net benefit from its interactions with the yeast, while the yeast neither receives a net benefit nor suffers a net loss from its interactions with the alga. Thus, according to this metric, yeast and alga form a net commensal relationship. However, we emphasize that this net commensalism is a result of a balance between the underlying competitive and cooperative interactions.

The fact that both yeast and alga can grow in our conditions alone or together allows us to enquire how evolution of one species is affected by its ecological interactions with the other in an otherwise identical

environment. We focus on the initial phase of adaptive evolution. As the yeast is likely to adapt faster than the alga (Supplementary Information, Section 1.2), we characterize the distribution of ecological and fitness effects of adaptive mutations arising in yeast and examine how these distributions depend on the presence/absence of the alga.

Alga alters yeast evolution without fitness trade-offs

We first asked whether and how ecological interactions with the alga change the distribution of fitness effects of adaptive mutations arising in yeast. To this end, we carried out five replicate BLT experiments in yeast evolving alone (the 'A condition') and in a community with the alga (the 'C condition'; Methods). In each population, we tracked the frequencies of ~5×10^5 neutral DNA barcodes integrated into the yeast genome[40] for 17 growth and dilution cycles. We identified on average 2,820 and 2,905 adapted barcode lineages per population in A and C conditions, respectively (Methods, Extended Data Figs. 2 and 3 and Supplementary Figs. 1–8). The similarity of these numbers suggests that the presence of the alga does not dramatically change the rate at which beneficial mutations arise in yeast.

Each adapted lineage is expected to initially carry a single beneficial driver mutation[37,38]. Thus, by tracking barcode frequencies, we can estimate the competitive fitness benefits of many simultaneously segregating driver mutations relative to the ancestral yeast strain (Methods). The estimated distributions of fitness effects of beneficial mutations (bDFEs) are much broader than expected from measurement noise alone in both A and C conditions (Supplementary Information, Section 1.4), indicating that yeast has access to multiple mutations with different fitness benefits, consistent with previous work[37,41]. Furthermore, the presence of the alga reduces the bDFE median (1.60 in A versus 1.50 in C; $P < 10^{-4}$, two-sided permutation test; Methods) and increases its width (interquartile range 0.31 in A versus 0.37 in C; $P < 10^{-4}$, two-sided permutation test; Fig. 2a and Supplementary Figs. 6 and 7). This increase in width is associated with the appearance of two peaks with higher relative fitness values around 2.0 and 2.5 (Fig. 2a and Supplementary Fig. 6). As the dynamics of adaptation depend on the shape of the bDFE[42,43], these results indicate that the presence of the alga alters evolutionary dynamics in the yeast population.

The presence of the alga can alter the yeast bDFE by changing which mutations are beneficial (that is, by imposing a fitness trade-off relative to the A condition) or by changing the fitness benefits provided by adaptive mutations, or both. To discriminate between these possibilities, we randomly sampled 221 yeast clones from distinct adapted lineages in the A condition ('A mutants') and 189 yeast clones from distinct adapted lineages in the C condition ('C mutants'). Clones were sampled at cycle 9, a timepoint at which most adapted lineages are expected to still be driven by a single beneficial mutation (Methods). We then used competition assays to measure the fitness of all A and C mutants relative to their ancestor in both A and C conditions (Methods, Supplementary Figs. 9–11 and Supplementary Data 2). These direct measurements of competitive fitness are concordant with our estimates from the BLT experiment (Supplementary Information, Section 2, and Supplementary Fig. 12). We found that the C mutants had significantly higher fitness in their 'home' C condition than A mutants, by on average 10.8% (95% CI 7.7–14.0%, $P = 2 \times 10^{-11}$, ANOVA model: fitness ~ environment, $F = 45.83$, df = 1) and that A mutants were more fit in their home A condition than C mutants by on average 14.4% (95% CI 10.2–18.5%, $P = 2 \times 10^{-11}$; $F = 45.42$, df = 1), consistent with local adaptation. However, the fitness distributions of both A and C mutants are wide and overlapping in both conditions, so that some A mutants are more fit than some C mutants in the C condition and vice versa.

Interactions with the alga significantly alter the fitness of 88% (362/410) of all sampled mutants (false discovery rate (FDR) 11%, obtained by permutation). However, fitness is positively correlated between the two conditions across all mutants (Fig. 2b; Pearson $R = 0.70$, 95% CI 0.65–0.75, two-sided $P = 10^{-63}$, $t = 19.9$, df = 408). Importantly, none of the A or C mutations is deleterious in their 'non-home' condition. Thus, the presence of the alga changes the fitness benefits provided by adaptive mutations in yeast but does not impose a measurable fitness trade-off, in the sense that it does not alter which mutations are beneficial.

Alga alters mutations contending for fixation in yeast

Given that all sampled yeast mutants are beneficial both in the presence and in the absence of the alga and that mutant fitness is correlated between the two conditions, we expected that the sets of A and C mutants would be genetically indistinguishable. To test this expectation, we sequenced the genomes of 181 out of 189 C mutants, 215 out of 221 A mutants, as well as 24 ancestral isolates as controls (Methods, Supplementary Figs. 13–16 and Supplementary Data 3). We found 176 large copy-number variants (CNVs) across 14 loci in the genomes of A and C mutants and none in the ancestral isolates. All of these large CNVs are thus probably adaptive (for an extended discussion, see Supplementary Information, Section 3), with a typical A and C mutant carrying on average 0.39 ± 0.04 and 0.51 ± 0.04 of these mutations, respectively. In total, 85/176 large CNVs are whole-chromosome aneuploidies. This large number of aneuploidies is consistent with the fact that they occur in *S. cerevisiae* at a rate of about 10^{-4} per diploid genome per generation[44] and the fact that they can be adaptive in some conditions[45–47]. Out of 91 remaining CNVs, 64 are partial losses on chromosome IV, with breakpoints concordant with known long terminal repeat elements (Supplementary Data 3).

In addition to large CNVs, we discovered 185 small indels and point mutations at 63 loci for which mutations are found in A and C mutants significantly more often than expected by chance (Supplementary Information, Section 3.2), suggesting that these small mutations are also adaptive. A typical A and C mutant carries on average 0.35 ± 0.03 and 0.60 ± 0.06 of these small adaptive mutations, respectively. Overall, we identified 361 beneficial mutations across 77 loci in 250 out of 396 adapted mutants, with each A and C mutant carrying on average 0.74 ± 0.04 and 1.11 ± 0.07 such mutations, respectively (Supplementary Table 2 and Supplementary Data 3).

To compare the diversity of adaptive mutations carried by A and C mutants, we calculated the probability that two random clones share a mutation at the same driver locus (P_g, where smaller P_g implies higher diversity). We found that P_g is statistically indistinguishable between the A mutants and C mutants ($P_g = 6.0 \pm 0.6\%$ and $8.5 \pm 0.8\%$, respectively; $P = 0.06$, two-sided permutation test; Methods). Nevertheless, there are large differences in the frequency distribution of driver mutations among A and C mutants (Fig. 2c, Extended Data Fig. 4 and Supplementary Data 4; $P = 5 \times 10^{-8}$, two-sided χ^2-test, $\chi^2 = 160.51$, df = 76), contrary to what we expected a priori.

This difference suggests that the chance for any given beneficial mutation to rise to a high enough frequency and be sampled varies dramatically between A and C conditions. For example, 10% (18/181) of C mutants carry a chrXIV-3n mutation, but none of the 215 A mutants does (Fig. 2c and Extended Data Fig. 4), despite the chrXIV-3n mutations being beneficial in both conditions (Fig. 2a,b). This initially puzzling observation could be explained by the dynamics of adaptation in populations evolving in the clonal interference regime[42,48,49]. Clonal interference prevents weak and/or rare beneficial mutations from reaching even moderately high frequencies[32,42,50,51]. Thus, the same beneficial mutation can have dramatically different chances of being sampled in the two conditions if it is located in different parts of the respective bDFEs. Consistent with this explanation, we find that a typical chrXIV-3n mutant is 2.05 ± 0.04 times more fit per cycle than the ancestor and ranks in the top 11 ± 1.3% of most fit mutants in the C condition, while being only 1.59 ± 0.03 times more fit than the ancestor and ranking at 53 ± 5.3% in the A condition (Fig. 2a). Other mutations with strong discrepancies in their representation among A and C mutants show similar shifts in their fitness effects and rank order (Fig. 2a and

https://doi.org/10.1038/s41559-022-01923-8

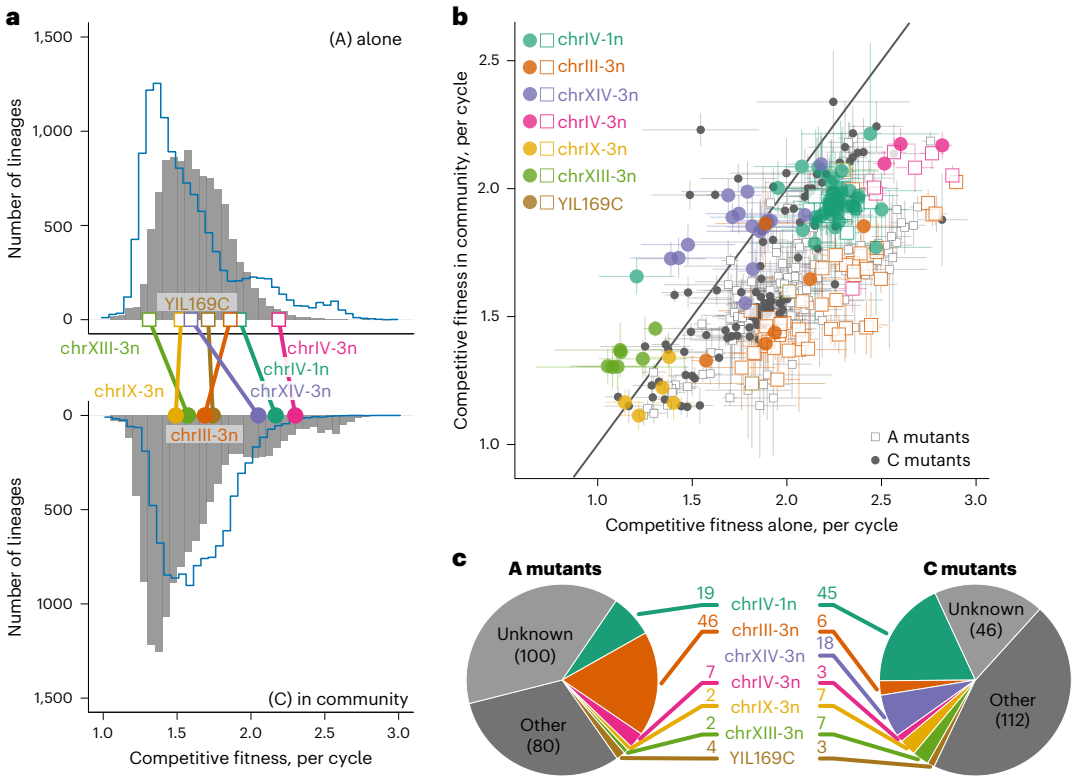

Fig. 2 | The presence of the alga affects adaptation in yeast at the fitness and genetic levels. a, Yeast bDFE when evolving alone (top) and in community with the alga (bottom). Each histogram is constructed from data pooled across five replicate BLT experiments. Blue outlines show the bDFE in the other condition. Each coloured point indicates the average fitness of a mutant carrying a mutation at the indicated driver locus (same data as in **b**). Large CNVs are referred to as chr*x*-*y*n, where *x* is the chromosome number and *y* is the number of copies. **b**, Fitness of A and C mutants ($n = 221$ and 189, respectively) measured in competition assays in the A and C conditions. Mutants carrying mutations at the seven most common driver loci are coloured. Data values are presented as means of three replicate measurements ±1 s.e.m. The solid line indicates the diagonal. **c**, Distribution of adaptive mutations among A and C mutants. Seven most common driver loci are shown individually; all other mutations are grouped into 'Other' (for full distributions, see Supplementary Data 3). Adaptive mutations that are expected to be present in our mutants but were not identified in the genome data are labelled as 'Unknown' (for details, see Supplementary Information, Section 3). Numbers indicate how many A and C mutants carry each type of driver mutation.

Supplementary Data 4). In general, the alga shifted the fitness ranks of mutants by 14.1 ± 0.8% on average. We used simulations to confirm that such differences in fitness effect and rank are sufficient to explain the observed differences in the genetic composition of A and C mutants (Supplementary Information, Section 4, and Extended Data Fig. 5).

The fact that the sets of A and C mutants are genetically different implies that the yeast populations in these two conditions are about to embark on distinct evolutionary trajectories. Indeed, A and C mutants primarily represent high-frequency lineages in the respective populations. Therefore, the mutations that they carry are more likely to win the clonal competition towards fixation in the condition from which they were sampled. Then, the fact that A and C mutants carry statistically distinct sets of mutations implies that mutations contending for fixation in yeast in the A versus C conditions are different. Therefore, by altering the fitness benefits of mutations, ecological interactions with the alga change the short-term evolutionary trajectory of yeast.

Yeast adaptations have diverse ecological consequences

A mutation that spreads and fixes in the yeast population could subsequently alter the ecological dynamics of the yeast–alga community, and adaptive mutations at different loci may have different ecological consequences. For example, some mutations could increase yeast's competitive ability and ultimately lead to the exclusion of the alga from the community. Others could increase yeast's cooperativity and thereby strengthen the mutualism. To assess the prevalence and the magnitude of different ecological effects of adaptive mutations in yeast, we selected 28 C mutants and 31 A mutants that are representative of the genetic diversity of contending mutations (Methods). We then formed 59 'mutant communities' by culturing each of these mutants with the alga ancestor. We quantified the ecological effect of each mutation by measuring yeast and alga yields in the mutant communities and alone and comparing their ratios (Methods and Supplementary Figs. 18 and 19).

We found that many of the adaptive mutations significantly affected both YYA and YYC (Fig. 3a and Supplementary Fig. 19a,b). Fifty-three per cent (31/59) of them significantly decrease YYA while 15% (9/59) of them significantly increase it (two-sided FDR 28%; Methods). At the same time, we found no mutations that significantly decreased YYC, but 34% (20/59) of them significantly increased it (FDR 26%). Mutations have uncorrelated effects on YYA and YYC (Fig. 3a), suggesting that yeast yield in the two conditions is determined by different underlying traits. Mutations in yeast also significantly alter AYC, with 24% (14/59) of mutations increasing it and 8% (5/59) decreasing it (FDR 32%), with the effects on AYC and YYC being positively correlated (Fig. 3b).

The fact that mutations alter the yields suggests that some of them may also tip the balance between cooperation and competition in one or the other direction. Indeed, we found that 24% (14/59) of mutants have significantly increased both AYC/AYA and YYC/YYA ratios, 39% (23/59) have a significantly increased the YYC/YYA ratio only, and 12% (7/59) have significantly decreased one or both ratios (two-tailed FDR 5%, Fig. 3c). Thus, 7 mutations strengthen the competition, and 37 mutations strengthen the mutualism.

https://doi.org/10.1038/s41559-022-01923-8

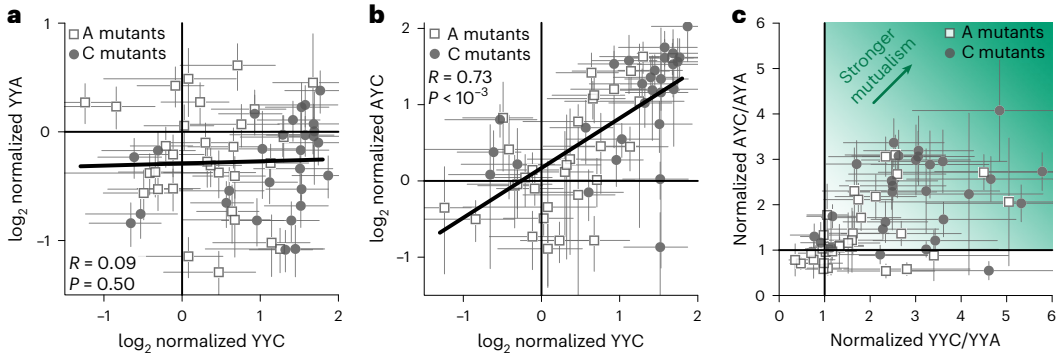

Fig. 3 | Adaptive mutations in yeast have diverse ecological consequences. **a**, Pearson correlation between YYC and YYA, normalized by ancestral values, across sampled mutants. **b**, Pearson correlation between YYC and AYC, normalized by ancestral values, across sampled mutants. **c**, The ratio of YYC to YYA and the ratio of AYC to AYA, normalized by ancestral values, across sampled mutants. Darker shades of green indicate stronger mutualism. For all panels, $n = 31$ for A mutants and $n = 28$ for C mutants with two replicate measurements, error bars represent ±1 s.e.m. In **a** and **b**, solid lines are fitted by linear regression, and two-tailed P values for the correlation coefficient are calculated by permutation (Methods).

These results show that yeast has access to beneficial mutations with ecologically diverse consequences and suggest that our community has the potential to embark on a variety of eco-evolutionary trajectories with possibly different ecological outcomes.

Alga biases selection towards mutualism-enhancing mutations

We next asked whether mutations contending for fixation in the presence and absence of alga have distinct ecological effects. We noticed that the C mutants clustered in the top right corner of the YYC-versus-AYC plot (Fig. 3b). Indeed, YYC and AYC values for the C-mutant communities are on average 103% and 79% higher than those for the A-mutant communities, respectively (YYC: 95% CI 62–143%, $P = 3 \times 10^{-4}$, permutation test; AYC: 95% CI 35–122%, $P = 4 \times 10^{-3}$; $n_1 = 28$ C mutants and $n_2 = 31$ A mutants). These differences remain large and significant even after accounting for the frequencies with which different driver mutations are observed in our yeast populations (YYC: $P = 10^{-5}$; AYC: $P = 3 \times 10^{-3}$, permutation test; Extended Data Fig. 6 and Methods), indicating that this clustering is not an accidental byproduct of our choice of A and C mutants. Instead, the observed differences in yield must be caused by systematic genetic differences between the A and C mutants. In other words, in the presence of the alga, natural selection favours yeast mutants that produce higher yields in the community. This conclusion is further corroborated by the fact that both YYC and AYC are correlated strongly and significantly with competitive fitness in the C condition, but only weakly with fitness in the A condition (Extended Data Fig. 7).

A mutation in yeast that increases YYC may concomitantly increase or decrease YYA (Fig. 3a), thereby increasing or decreasing the net benefit that yeast derives from its interactions with the alga. We found that 86% (24/28) of the C mutants had a significantly higher YYC/YYA ratio than the ancestor (FDR 21%), of which 32% (9/28) had also a significantly higher AYC/AYA ratio (FDR 6%; Fig. 3c), but only 1/28 had a significantly lower AYC/AYA ratio (FDR 58%). In contrast, only 52% (16/31) of the A mutants had a higher YYC/YYA ratio (FDR 35%), of which 16% (5/31) also had a higher AYC/AYA (FDR 12%) and 2/31 had lower AYC/AYA (FDR 29%). Thus, C mutants both more often benefit from the alga and provide benefits to the alga compared with the A mutants. In other words, more adaptive mutations that dominate yeast adaptation in the presence of the alga strengthen the mutualism by increasing yeast cooperativity and/or decreasing its competitiveness, compared with mutations that dominate adaptation in the absence of the alga.

An interesting potential consequence of this shift in selection on yeast precipitated by the presence of the alga is that it can change the repeatability of yeast evolution along the competition–mutualism continuum. We quantified such ecological repeatability by the probability that two randomly drawn yeast mutants that contend for fixation in a given condition both increase or both decrease the YYC/YYA ratio and simultaneously both increase or both decrease the AYC/AYA ratio. The probability of ecological parallelism would be 25% under a uniform null model. For the A mutants, this probability is 33 ± 2.8%, indistinguishable from the null expectation ($P = 0.21$, two-sided χ^2 test, $\chi^2 = 1.55$, df = 1). In contrast, it is 68 ± 5.5% for the C mutants, which is significantly higher than expected ($P = 6 \times 10^{-8}$, $\chi^2 = 29.3$, df = 1) and also significantly higher than for the A mutants ($P = 0.031$, two-sided permutation test; Methods). Thus, yeast evolves more repeatably (towards stronger mutualism) in the presence of the alga than in its absence.

In summary, our results show that mutations contending for fixation in yeast populations evolving alone have relatively diverse effects on the ecology of the yeast–algal community, with some strengthening and some weakening the mutualism. In contrast, mutations contending for fixation in yeast evolving with the alga predominantly lead to higher yields of both species, which strengthens the yeast–alga mutualism and makes evolution more repeatable at the ecological level.

Selection does not directly favour mutualism enhancement

We next asked how stronger mutualism could possibly evolve in our community. Specifically, does natural selection in the presence of the alga favour mutations that increase cooperativity and/or decrease competitiveness in yeast directly, or is this bias a byproduct of selection for other traits[25,52]? Natural selection can directly favour rare mutualism-enhancing (that is, more cooperative and/or less competitive) yeast mutants only if such mutants preferentially receive fitness benefits from their algal partners, that is, if there is a partner-fidelity feedback[53]. Our system is well mixed, so that all diffusible benefits are shared by the entire culture, eliminating any potential fitness advantage of rare mutualism-enhancing mutants[25,54]. The only way to ensure preferential benefit exchange with an algal partner under well-mixed conditions is for a cooperative mutant to form a physical association with its partner[21]. However, we found no evidence for such associations in any of the sampled mutants (Extended Data Fig. 8 and Methods). Given the absence of a plausible partner-fidelity feedback, the increased cooperativity and/or decreased competitiveness of the C mutants must be a byproduct of selection for one or more other traits.

We sought to identify traits under selection in the C condition that could cause yields to increase. Both competitive fitness and yield depend on fundamental physiological and life-history traits embodied by yeast and alga, such as their growth rates, mortalities, nutrient consumption efficiencies and so on[55]. We focused on two key traits that are known to be under selection in environments with variable

https://doi.org/10.1038/s41559-022-01923-8

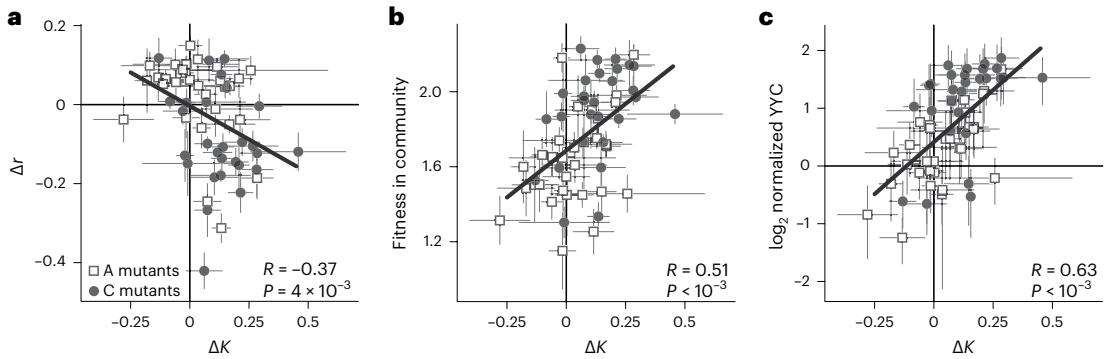

Fig. 4 | The effects of adaptive mutations on life-history traits, fitness and yield. The effects of mutations on growth rate (r) and peak density (K) in the A condition, Δr and ΔK, are reported as fractional differences relative to the ancestral values (Methods). **a**, Pearson correlation between ΔK and Δr among all sampled adapted mutants. **b**, Pearson correlation between ΔK and competitive fitness in the community among all sampled adapted mutants. **c**, Pearson correlation between ΔK and YYC, normalized to ancestral values, among all sampled adapted mutants. Error bars show ±1 s.e.m. Solid lines are fitted by linear regression. $n = 31$ for A mutants and $n = 28$ for C mutants, with two replicate measurements for ΔK, Δr and YYC and three replicate measurements for fitness. Two-tailed P values for the correlation coefficient are calculated by permutation (Methods).

nutrient availability, namely, the maximum population growth rate, r, and the carrying capacity, K. r is important for competitive fitness when resources are abundant[56,57], a condition that takes place at the beginning of each growth cycle in our cultures. K is important for competitive fitness when resources are scarce[56,57], a condition that takes place at the later phase of each growth cycle. We measured r and K in the A condition, reasoning that these intrinsic traits would be relevant for fitness and yield in both A and C conditions. We estimated r by regressing the natural logarithm of the yeast cell density against time during the initial phase of the growth cycle (Methods). We estimated K as the maximum yeast cell density during the growth cycle, which is usually achieved on day 2.

We measured r and K for all 59 sampled mutants (Supplementary Figs. 20 and 21 and Methods) and found that many mutations significantly affected either one or both traits (Fig. 4a). We found a negative correlation between the effects of mutations on r and K (Pearson $R = -0.38$, 95% CI −0.59 to −0.13, two-sided permutation $P = 0.004$; Fig. 4a), indicating a commonly observed trade-off between growth rate and nutrient utilization efficiency[58–65]. In particular, we found 16 C mutants and 4 A mutants having a significantly higher K and a significantly lower r than the ancestor (FDR 18%), an observation that is rare in experimental evolution studies[60] where selection usually favours higher r (refs. [55,59,66–69]). However, theory suggests that high-K/low-r mutations can be favoured in the presence of an r–K trade-off in populations near starvation[56,57]. We confirmed that 60% (12/20) of our significant high-K/low-r mutants can in fact invade the ancestral yeast population in simulations of a logistic growth model (Supplementary Information, Section 5.2, and Supplementary Fig. 22). While this model demonstrates the plausibility of selection favouring high-K/low-r mutants, it does not capture all the important complexities of our system. To test whether r and K are under selection in our A and C conditions, we next examined the correlation between these traits and competitive fitness among all 59 assayed mutants.

We found that neither r nor K is significantly correlated with fitness in the A condition (Supplementary Information, Section 5.3, Extended Data Figs. 9b and 10a and Supplementary Table 4). As a result, the A mutants have r and K values that are indistinguishable from the ancestor (average $\Delta r = 2 \pm 1.9\%$, $P = 0.27$; average $\Delta K = 3 \pm 2.4\%$; $P = 0.29$; $n = 31$, permutation test). These observations suggest that other traits that we have not measured must be more important for fitness in the A condition than either r or K.

In contrast, fitness in the C condition is positively correlated with K (Fig. 4b, $R = 0.51$, 95% CI 0.29–0.68, $P < 10^{-4}$) and negatively correlated with r (Extended Data Fig. 9a; Pearson's $R = -0.51$, 95% CI −0.68 to −0.29, $P < 10^{-4}$), consistent with the observed r–K trade-off. Both traits together explain 37% of variation in competitive fitness in the C condition. Interestingly, a negative correlation between fitness and r persists even after controlling for K (Supplementary Table 4), suggesting that other unmeasured traits that exhibit a trade-off with r must also be important for fitness in the C condition. Regardless, C mutants reach K values on average 12.7% higher than the ancestor ($P = 4 \times 10^{-4}$, permutation test) and 9.5% higher than A mutants (95% CI 2.6–16.3%, $P = 0.03$). A typical C mutant also has a significantly lower r than both the ancestor (average $\Delta r = -8.7 \pm 2.3\%$, $P = 0.001$) and a typical A mutant ($\Delta r = -11\%$, 95% CI −17.0% to −5.1%, $P = 7 \times 10^{-4}$). These observations suggest that nutrient efficiency is an important component of fitness in the C condition and that high-K/low-r yeast mutants are favoured by selection in the presence of the alga.

We next asked whether higher-K mutants achieve higher yields. We might expect a strong positive correlation between these quantities because, all else being equal, mutants that reach higher density in the middle of the growth cycle owing to their higher carrying capacity are more likely to maintain higher density at the end of the growth cycle. However, we found no correlation between K and YYA (Extended Data Fig. 10c), which suggests that adaptive mutations must affect other unmeasured traits that are more important than K for yield in the absence of the alga. In contrast, we found that K and YYC were positively correlated (Fig. 4c), suggesting that higher nutrient efficiency is important for achieving higher yields in the community with the alga.

Our observations suggest a plausible model for how adaptive evolution can favour mutualism enhancement in the absence of partner-fidelity feedbacks: ecological interactions with the alga intensify selection for yeast mutants that use resources more efficiently (that is, those that reach higher K even at the expense of reduced r); once these mutants spread in the yeast population, they support higher yields of both members of the community. Whether mutualistic partners generally induce selection for lower r and/or higher K, and whether such selection consistently leads to increased yields of both species, remains an open question.

Finally, similarly to our analysis of ecological parallelism, we asked whether the presence of the alga alters the probability of trait parallelism, which we define as the probability that both r and K would be affected in the same direction in two randomly sampled mutants (Methods). We find that the probability of trait parallelism is 30.7 ± 1.7% for the A mutants, which is not significantly different from 25% expected under the uniform null model ($P = 0.47$, two-sided χ^2 test, $\chi^2 = 0.53$, df = 1). In contrast, the probability of trait parallelism is 46.3 ± 4.8% for the C mutants, which significantly exceeds 25% ($P = 0.009$, $\chi^2 = 6.7$,

df = 1), suggesting that evolution in the presence of the alga becomes more repeatable not only at the ecological level, as shown in the previous section, but also at the level of underlying life-history traits.

In summary, our results show that interactions with alga shift natural selection on yeast to favour mutants that increase *K* and decrease *r*, which in turn leads to increased yields of both species in the community. The shift in selection imposed by the alga makes evolution more repeatable both at the level of life-history traits and even more so at the ecological level.

Discussion

We characterized early adaptation in the experimental yeast–alga community and made three main observations. First, we found that yeast has access to adaptive mutations that are not only genetically diverse but also have diverse ecological effects. Second, even though there are no measurable fitness trade-offs for yeast between growing alone or with the alga, the presence of the alga modifies the fitness benefits provided by many mutations. This shift in selection pressures is sufficient to change the set of mutations that contend for fixation in yeast and thereby to alter the course of its evolution. Third, mutations that are strongly favoured by selection in the presence versus absence of the alga have different ecological consequences. Specifically, the presence of the alga shifts selection on yeast to favour mutations that enhance the yeast–alga mutualism (as measured by the yield of both species at the end of the growth cycle), making evolution at the ecological level more repeatable.

Insofar as our yeast–alga community is representative of other ecological communities, our results suggest that (1) organisms have access to a variety of adaptive mutations with diverse ecological consequences and (2) ecological perturbations, such as removal or addition of species, can change the fitness effects of many of these mutations, thereby altering future outcomes of evolution not only at the genetic but also at the ecological level. As a result, the eco-evolutionary dynamics of multi-species communities are probably historically contingent on both prior evolution[70] and ecology[71]. Thus, we might expect that ecological communities would generically have the potential to embark on a variety of divergent eco-evolutionary trajectories and approach different ecological attractors. For example, mutations that are beneficial to yeast in our community can either increase or decrease the yields of both species suggesting that our community has the potential to evolve either towards stronger mutualism or towards mutualism breakdown, with probabilities of these outcomes being dependent on whether yeast previously evolved in the presence or absence of the alga.

Given this potential for ecological and evolutionary historical contingency, one might expect a priori that replicate communities would often diverge towards different ecological states. However, recent laboratory studies have found that replicate communities tend to evolve towards similar ecological states with notable repeatability[13,15,16,20,21,24,25,72–76]. Our results show that, while yeast has access to a set of adaptive mutations that are quite diverse in terms of their ecological effects, natural selection acting on yeast growing in the community strongly favours a biased subset of these mutations, namely, those that produce higher yields of both yeast and alga. When viewed in the context of these prior observations, our findings suggest that ecological interactions may limit the space of the most likely evolutionary trajectories. In our system in particular, the presence of the alga modifies the effects of mutations in yeast in such a way that yeast evolution becomes more repeatable at the ecological level, at least over the short term. In other words, ecological interactions may canalize evolution. Whether such canalization is a general feature of evolution in a community context remains to be determined.

In our competitive mutualistic community, canalization appears to occur in the direction of enhanced mutualism in the sense that the presence of the alga shifts selection on yeast in favour of mutations that benefit both species. There are no demonstrated mechanisms that would directly favour such enhanced mutualism in our community, but our results suggest another plausible scenario for how it can evolve. Mutations in yeast favoured in the presence of the alga tend to increase yeast's carrying capacity in our medium and reduce its growth rate. Increased carrying capacity could provide the competitive advantage necessary for such mutants to spread. Once these mutations dominate, increased *K* and/or decreased *r* could enhance cooperation or reduce competition with the alga. Specifically, increased *K* implies that there are more yeast cells to generate CO_2, which stimulates algal growth. Reduction in *r* could also benefit the alga via the 'competitive restraint' mechanism[77] in which slower-growing yeast compete less for the initial supply of ammonium and thereby offer the alga an opportunity to grow more and supply more ammonium during the latter portions of the growth cycle. However, competition for the initial ammonium can probably not be reduced to zero solely by mutations in yeast because yeast lacks the molecular machinery for metabolizing the only other nitrogen source, nitrite. Therefore, a single mutation or even a few mutations cannot alleviate yeast's basic requirement for ammonium. Furthermore, traits other than *r* and *K* most certainly contribute to both fitness and yield. Thus, additional experiments will be needed to determine how adaptive mutations in yeast modify the competitive and cooperative phases of the growth cycle to provide an evolutionary advantage and increase the yields of both species.

How the presence of the alga amplifies the fitness advantage of high-*K* mutants is currently unclear. An analysis of the genetic and biochemical basis of yeast adaptation may help us answer this question and assess how general the ecological mechanisms of mutualism enhancement might be. However, one challenge is that many mutations driving adaptation in yeast are large chromosomal amplifications and deletions, and it is unclear which amplified/deleted genes actually cause the fitness gains and changes in the ecologically relevant traits. At this point, we can only speculate on this subject. For example, it is known that ChrXIV-3n amplifications are adaptive under ammonium limitation, possibly driven by the copy number of the gene *MEP2*, which encodes a high-affinity ammonium transporter[78]. We suspect that these adaptations are particularly beneficial to yeast in the C condition because the alga provides a continuous but low flux of ammonia. Another interesting example are mutations in genes *HEM1*, *HEM2* and *HEM3*, which provide much larger fitness benefits in the C condition compared with the A condition (Supplementary Data 4) possibly because they shift the metabolic balance towards fermentation at higher concentrations of dissolved oxygen produced by the alga (Supplementary Information, Section 6). Elucidating these and other mechanisms of physiological adaptation in our competitive mutualistic systems is the subject of future work.

To conclude, our results suggest that microbial adaptation in the community context is driven by many mutations that are genetically and phenotypically diverse and have diverse ecological consequences. Changes in the ecological milieu, such as loss of some species or invasions by others, may not necessarily alter which mutations are beneficial to community members, but only quantitatively shift their fitness benefits. Such relatively subtle changes may nevertheless be sufficient for altering and canalizing evolutionary trajectories.

Methods

BLT experiment and data analysis

Strains. We used *C. reinhardtii* strain CC1690. The barcoded library of the diploid yeast *S. cerevisiae* strain GSY6699 (ref. [40]) was kindly provided by Prof. Gavin Sherlock. This is a diploid, prototrophic strain derived from the BY genetic background, homozygous throughout the genome, except for locus YBR209W, where one copy of a DNA barcode was integrated[37]. Our starting library consists of about 5×10^5 clones that carry unique DNA barcodes at this locus and are otherwise genetically identical (for a discussion of pre-existing polymorphisms, see Supplementary Information, Sections 1.3 and 3).

Growth conditions. Both yeast monocultures and yeast–alga communities were cultured in a defined minimal medium[33] ('CYM medium') supplemented with 2% dextrose, 10 mM KNO_2 and 0.5 mM NH_4Cl, which we thereafter refer to as 'growth medium'. All cultures were grown in 10 ml of growth medium in 50 ml flasks (Fisher Sci #FS2650050) capped with 50 ml plastic beakers (VWR #414004-145) at room temperature (21 °C) on a platform shaker with 70 foot-candles of constant light (three Feit Electric #73985 suspended approximately 24 inches above the platform shaker) shaking at 125 r.p.m., unless noted otherwise.

BLT pre-cultures. Before the BLT experiment, yeast and alga were pre-cultured in 50 ml of growth medium in 250 ml delong baffled flasks (PYREX #C4446250) for 2 and 10 days, respectively. Alga pre-cultures were started from colonies. Pre-cultures of barcoded yeast libraries were started from frozen stocks by transferring 500 µl into 50 ml of the growth medium.

BLT initiation and propagation. We conducted five replicate BLT experiments for each of two treatments, yeast alone (the A condition) and yeast + alga community (the C condition). Each BLT experiment in the A condition was initiated from 100 µl of the yeast pre-culture. Each community BLT experiment was initiated from 100 µL of the 1:1 (v/v) yeast and alga mixture. Cultures were grown for 5 days before being diluted 1:100 for the next growth cycle (100 µl into 10 ml fresh medium). A total of 17 growth/dilution cycles were completed.

Culture preservation. Glycerol stocks were taken of the yeast pre-culture and yeast + alga inoculum mixtures, as well as at the end of every odd growth cycle. Separate stocks were stored for DNA extraction and cell isolation purposes with two replicates each, for a total of four stocks per culture per timepoint. Cell isolation stocks were created by aliquoting 1.5 ml of culture into 500 µl of 80% glycerol, mixing by vortex and storing at −70 °C. DNA stocks were created by removing the supernatant of the remaining 7 ml of culture via centrifugation and resuspending in 2 ml of 20% glycerol (80% glycerol diluted with 1× PBS), which was then stored as two separate 1 ml stocks at −70 °C.

Sequencing and analysis. DNA was isolated and the amplicon sequencing libraries of the barcode locus were prepared using standard methods (Supplementary Information, Section 1.3). The analysis of barcode data is described in Supplementary Information, Section 1.4.

Competitive fitness assays

We selected cycle 9 to isolate adapted mutants because the estimated fraction of adapted lineages in our evolving populations was large, but each adapted lineage was still at a low frequency (Extended Data Figs. 2 and 3). Specifically, 92% of a typical population in the A condition consisted of adapted lineages, with the median frequency of an individual adapted lineage being 9×10^{-5} (approximately nine cells per lineage at the bottleneck), and 73% of a typical population in the C condition consisted of adapted lineages, with the median frequency of an individual adapted lineage being 7×10^{-5} (approximately seven cells per lineage at the bottleneck).

Isolation of random clones. To isolate adapted clones, frozen stocks of the yeast A and C populations from cycle 9 were thawed, plated onto standard 100 mm Petri dishes with CYM + 1% agarose at a dilution of approximately 100 cells per dish, and incubated at 30 °C for 3 days (the alga does not grow at 30 °C). Eighty-eight random colonies were isolated from each population, that is, a total of 440 clones from the A and C condition each. Eight additional clones from each population were collected at cycle 17 and are present in the pools described below, but they are not included in any of the analyses presented in this study. Each colony was transferred into a well of a 96-well plate (Corning 3370) with 200 µl of CYM medium and incubated for 2 days at 30 °C. Then, 50 µl of 80% glycerol was added to each well, and the plate was stored at −70 °C.

Barcode genotyping. The DNA barcodes of all isolated clones were identified by sequencing, using the Sudoku method[79,80]. Specifically, 10 µl of each clone was pooled into 10 'population' pools (one pool for each source population), 8 'row' pools and 12 'column' pools. DNA barcodes in each pool were amplified and sequenced as described in Supplementary Information, Section 1.3. We expect that a given combination of row, column and population pools would have a single barcode in common, defining the isolate in the corresponding well of the appropriate plate. We determined all barcodes present in the intersection of each combinations of row, column and population pool. If only a single barcode is identified in the intersection, the corresponding well is assigned that barcode identity. If multiple barcodes or no barcode are identified, the associated clone is removed from further analysis.

Competition assay experiment. To conduct the competitive fitness assays, we pooled clones into three pools (N, A and C; Supplementary Information, Section 2) and pre-cultured each pool separately in the growth medium for 2 days. We also pre-cultured the alga for 10 days, starting from colonies. We then combined A, C and N pools in a 1:1:18 ratio. We carried out three replicate competitions in the A and C conditions each. To this end, we inoculated each replicate with 100 µl of the combined A/C/N pool. In addition, the three C-condition replicates were inoculated with 100 µl of the alga pre-culture (~10^6 cells ml^{-1}). All replicates were propagated in conditions identical to the BLT experiment for a total of five growth cycles. Glycerol stocks were made at the end of each growth cycle after the dilution step by centrifuging the culture, removing spent medium and resuspending the pellet in 2 ml of 20% glycerol + PBS. Two 1 ml aliquots of this glycerol suspension were stored at −70 °C. One of these aliquots was collected for DNA extraction and barcode sequencing (for methodological details, see Supplementary Information, Section 1.3).

Competition assay data analysis. Barcodes were identified and counted as described in Supplementary Information, Section 1.4. The resulting barcode count data were analysed as described previously[38] using software available at https://github.com/barcoding-bfa/fitness-assay-python. Briefly, the 84 non-adapted barcodes (as defined from the BLT analysis) from the N pool were used to estimate the mean fitness trajectories and the additive and multiplicative noise parameters for each pair of timepoints in each assay[38]. These estimates were used to estimate the fitness of every lineage for each pair of neighbouring timepoints and the noise parameter. The variance of an estimate for a given pair of timepoints was calculated as the inverse of the read depth at the earlier of the two timepoints + the estimated noise parameter. Inverse variance weighting was then used to combine estimates across all time point pairs to generate a single fitness and error estimate for each lineage in each replicate. Replicate estimates were combined using further inverse variance weighting to generate the final fitness estimate for each isolate in the A and C conditions. For each mutant in each condition, we also calculated the 95% confidence interval around the fitness estimate based on the variability in fitness measurements between replicates (assuming that measurement errors are distributed normally). Fitness estimates are provided on a per growth cycle basis. Validation of this analysis procedure and additional statistics are described in Supplementary Information, Section 2.

Genome sequencing and analysis

We sequenced full genomes of 219 A mutants, 187 C mutants, 8 non-adapted evolved isolates and 24 ancestral isolates sampled from the inoculum population. DNA was extracted using the YeaStar kit Protocol I (Zymo Research #D2002) with in-house produced YD Digestion buffer (1% SDS + 50 mM Na_2PO_4), DNA Wash buffer

(80% ethanol + 20 mM NaCl) and Elution Buffer (10 mM Tris–HCl). For each sample, 0.2 µl of 25 mg ml^{-1} RNAse A (Zymo Research #E1008-8) and 1 U (0.2 µl of 5 U µl^{-1} stock solution) of Zymolyase (Zymo Research #E1004) were used. Libraries were prepared using the method described by Baym et al.[81] and sequenced on the Illumina HiSeq4000 platform. Sequencing services were provided by Novogene and the UCSD Institute for Genomic Medicine. Sequencing failed for four A mutants and six C mutants, leaving us with 215 A mutants and 181 C mutants with sequenced genomes, 8 non-adapted evolved isolates and 24 ancestral isolates (a total of 428 clones). For these clones, we obtained high-quality genome data (>4× coverage, mean coverage of 24×). Variant calling, filtering and statistical analysis are described in detail in Supplementary Information, Section 3.

Probability of genetic parallelism. We calculate the probability of genetic parallelism P_g for a set of mutants as follows. We consider every pair of mutants and calculate the proportion that have a mutation in at least one common driver locus (including both small variants and CNVs). Adapted clones with no mutations at the identified driver loci are assumed to have an adaptive mutation at a locus that is not shared with any other isolate in the set. To test whether A and C mutants have different probabilities of genetic parallelism, we re-shuffle the evolution treatment label (that is, alone versus community) across all A and C mutants and calculate P_g for both resulting groups. We obtain the absolute value of the difference in P_g between the two groups, $|\Delta P_g|$, in 1,000 such permutations, and estimate the P value as the fraction of permutations where $|\Delta P_g|$ exceeds the observed difference.

Phenotyping

For all phenotypic measurements, replicate measurements were conducted using distinct samples. In no case was a single sample measured repeatedly.

Measurement of ancestral yeast and alga growth. Yeast and alga were thawed from frozen stocks (−70 °C for yeast, LN2 storage for algae) and grown separately in standard growth conditions for one growth cycle. Communities were inoculated by mixing 100 µl of yeast with 10^4 cells of alga into 10 ml of our growth medium and propagated for one cycle via 100-fold dilution. On the second growth cycle, each culture (yeast alone, alga alone and the community, with six replicates each) was characterized daily by colony-forming unit (CFU) counting for the yeast, and chlorophyll fluorescence measurements for the alga. Each culture was plated onto CYM medium plates (1% agarose) and incubated at 30 °C. Colonies were counted to estimate the density of yeast in each culture at each timepoint. We estimate alga density by measuring chlorophyll b fluorescence. To that end, we transfer 200 µl of each culture into a well of a black-wall clear-bottom 96-well plate (Corning #3631) and measure fluorescence in a plate reader (Molecular Devices Spectramax i3x, excitation at 435 nm and observation at 670 nm). Chlorophyll fluorescence intensity measurements were converted into cell density estimates as described in Supplementary Information, Section 5.1.

Selection of A and C mutants for phenotyping experiments. We selected 31 C mutants and 28 A mutants to cover a diversity of mutations and fitness values represented among all sampled adaptive mutants (Supplementary Data 4). Our reasoning for this non-random sampling was that mutants carrying a driver mutation at the same locus would have similar phenotypic values. If we selected clones for phenotyping randomly, we would have probably not observed more rare phenotypes. To account for this over-dispersion in the selection of mutants, we apply the mutation weighting procedure described below.

Measurement of YYA. To estimate YYA, we inoculated all 60 yeast strains (including the ancestor) individually into the standard conditions (10 ml of medium in 50 ml flasks) from frozen stocks and propagated them for two cycles (10 days). During the third cycle, we estimated yeast densities after 5 days of growth by plating and colony counting. Correlations between replicate measurements are shown in Supplementary Fig. 19a.

Measurements of YYC and AYC. We create mutant communities as follows. On day 0, we inoculate 50 ml growth medium (in 250 ml non-baffled Erlenmeyer flask) with 1 ml of CC1690 *C. reinhardtii* stock stored in LN2 and incubate for 20 days. On day 20, 100 µl of this culture is transferred to standard conditions (10 ml of fresh medium in a 50 ml flask). Also on day 20, the 60 yeast strains (including the ancestor) are individually inoculated into the standard condition from frozen stocks. On day 25, we form the mutant communities by transferring 100 µl of each yeast culture and 200 µl of the algae culture into fresh medium (200 µl of alga were used instead of 100 µl because the density of algae culture was approximately 50% of that at the initiation of the BLT experiment). These mutant communities are grown for one cycle in our standard conditions. On day 30, we transfer 100 µl of each mutant community into 10 ml fresh medium, as in the BLT experiment. We estimate both yeast and alga density on day 35. Yield estimates can be found in Supplementary Data 2. Correlations between replicate measurements are shown in Supplementary Fig. 19b,c.

Microscopy. To detect potential physical associations between alga and yeast mutants, we created mutant communities as described above. After 5 days of growth, communities were mounted on glass microscope slides (Fisher Scientific 12550143), sealed with Dow Corning high vacuum grease (Amazon B001UHMNW0) and imaged on a light microscope using a 40× objective with DIC. Extended Data Fig. 8 shows one representative community; the remaining 17 imaged mutant communities along with wild-type controls can be found in the Dryad data repository.

Mutant growth curve measurements. To estimate the growth parameters r and K for individual beneficial mutants, we measured growth curves of individual yeast mutants and the ancestor in the A condition. To this end, we inoculated all 60 yeast strains (including the ancestor) individually into the BLT condition (10 ml of medium in 50 ml flasks) from frozen stocks and propagated them for two cycles (10 days). During the third cycle, we estimated yeast densities on days 10, 10.5, 11, 11.5, 12, 13, 14 and 15 by plating and colony counting. We estimate r as the slope of the relationship between log(CFU ml^{-1}) and time (in hours) for the three measurements between 12 h and 36 h of growth. We estimate K as the maximum observed density (in CFU ml^{-1}). Data are provided in Supplementary Data 2. The growth curves are shown in Supplementary Fig. 20. Correlations between replicate measurements of r and K are shown in Supplementary Fig. 21.

Mutation weighting. Even though not all A or C mutants were phenotyped, we would like to make statistical statements about the distribution of phenotypes among all sampled A or C mutants. To this end, we associate each of the 59 phenotyped mutants with a single driver mutation. Mutants with multiple driver mutations are associated only with the most common driver mutation. Mutants with no identified driver mutations are associated with a unique unknown mutation. To obtain the prevalence of a given phenotypic value among all A or C mutants, we weight each measured phenotypic value by the number of sequenced A or C mutants with the same driver locus as the phenotyped mutant and divide by the total number of phenotyped A or C mutants.

Kernel density estimation. We use kernel density estimate to determine how likely certain phenotypic trait values would occur among all A and/or C mutants. Specifically, we obtain the kernel density estimates $D_A(y,a)$ and $D_C(y,a)$ for the probabilities that a community formed by

the ancestral alga and a random A or C mutant, respectively, would produce yeast yield y and alga yield a. To estimate D_A, we apply the kde2d function in R with bandwidth 1 along the x axis and 4/3 along the y axis to the mutation-weighted yield data for the A mutants. We analogously obtain $D_C(y,a)$.

Accounting for measurement errors in statistical tests by permutation testing. As the measurement errors in our estimates of r, K, yeast yield and alga yield are quite large, we use a permutation and resampling procedure to determine the statistical significance in various tests involving these variables. We permute isolate labels and resample the measurement values associated with each isolate from the normal distribution with the mean and the variance estimated for that isolate. We carry out 1,000 such simulations in each test. We estimate the expected false positive rate as the average fraction of resampled values significant at a chosen threshold per simulation. FDR is the average number of false positives divided by the number of observed positives.

Permutation tests of Pearson correlation significance are conducted as follows. For each permutation, isolate labels for each variable are permuted independently and phenotypic values are resampled as above. A randomized correlation coefficient is determined from each of the 1,000 permutations, and significance is determined by the proportion of randomized R^2 values that exceed the observed R^2 value.

Ecological and trait parallelism. We quantify the degree of parallelism among a set of mutants with respect to a pair of quantitative traits X and Y as follows. Suppose that one randomly picked mutant has trait increments ΔX_i and ΔY_i relative to the ancestor and another randomly picked mutant has trait increments ΔX_j and ΔY_j. We then estimate the probability that both $(\Delta X_i)(\Delta X_j) \geq 0$ and $(\Delta Y_i)(\Delta Y_j) \geq 0$. This measure of parallelism emphasizes the direction of change rather than the magnitude. When we compute this measure for the pair of yields of mutant communities, in which case X and Y are yeast and alga yields, we refer to it as the probability of ecological parallelism. When we compute this measure for the life-history traits, in which case X and Y are r and K, we refer to it as the probability of trait parallelism.

We obtain these probabilities of parallelism for the A and C mutants. We test the significance of the deviation of these probabilities from the expectation of 25% parallelism via a χ^2 test. To determine the statistical significance of the difference between the probabilities of parallelism for the A and C mutants, we resample the phenotypic values of each of the 59 mutants from the normal distribution (see above) and permute mutant genotype and home-environment labels, so that the genotype and label are always associated with each other but dissociated from the phenotypic values. We then calculate the parallelism probabilities for these permuted and resampled data. We estimate the P value by carrying out this permutation and resampling procedure 1,000 times.

Reporting summary

Further information on research design is available in the Nature Research Reporting Summary linked to this article.

Data availability

All raw sequencing data are available on the US National Center for Biotechnology Information (NCBI) Sequence Read Archive (SRA) under BioProject PRJNA735257. Other input data can be found on Dryad[82]. Strains and other biological materials are available by request to S.K. Source data are provided with this paper.

Code availability

The latest version of the barcode counting software BarcodeCounter2 is available at https://github.com/sandeepvenkataram/BarcodeCounter2.git. Analysis scripts, including the version of BarcodeCounter2 used in this study, can be found on Dryad[82].

References

1. Agostini, S. et al. Ocean acidification drives community shifts towards simplified non-calcified habitats in a subtropical–temperate transition zone. *Sci. Rep.* **8**, 11354 (2018).
2. Walther, G.-R. et al. Ecological responses to recent climate change. *Nature* **416**, 389–395 (2002).
3. Gilbert, B. & Levine, J. M. Ecological drift and the distribution of species diversity. *Proc. Biol. Sci.* **284**, 20170507 (2017).
4. White, E. P. et al. A comparison of the species–time relationship across ecosystems and taxonomic groups. *Oikos* **112**, 185–195 (2006).
5. Sax, D. F. & Gaines, S. D. Species invasions and extinction: the future of native biodiversity on islands. *Proc. Natl Acad. Sci. USA* **105**, 11490–11497 (2008).
6. Thompson, J. N. Rapid evolution as an ecological process. *Trends Ecol. Evol.* **13**, 329–332 (1998).
7. Post, D. M. & Palkovacs, E. P. Eco-evolutionary feedbacks in community and ecosystem ecology: interactions between the ecological theatre and the evolutionary play. *Philos. Trans. R. Soc. Lond. B* **364**, 1629–1640 (2009).
8. Reznick, D. N. & Travis, J. Experimental studies of evolution and eco-evo dynamics in guppies (*Poecilia reticulata*). *Annu. Rev. Ecol. Evol. Syst.* https://doi.org/10.1146/annurev-ecolsys-110218-024926 (2019).
9. Hendry, A. P. *Eco-evolutionary Dynamics* (Princeton Univ. Press, 2020).
10. Schoener, T. W. The newest synthesis: understanding the interplay of evolutionary and ecological dynamics. *Science* **331**, 426–429 (2011).
11. Yoshida, T., Jones, L. E., Ellner, S. P., Fussmann, G. F. & Hairston, N. G. Rapid evolution drives ecological dynamics in a predator–prey system. *Nature* **424**, 303–306 (2003).
12. Hansen, S. K., Rainey, P. B., Haagensen, J. A. J. & Molin, S. Evolution of species interactions in a biofilm community. *Nature* **445**, 533–536 (2007).
13. Hillesland, K. L. & Stahl, D. A. Rapid evolution of stability and productivity at the origin of a microbial mutualism. *Proc. Natl Acad. Sci. USA* **107**, 2124–2129 (2010).
14. Turcotte, M. M., Reznick, D. N. & Hare, J. D. The impact of rapid evolution on population dynamics in the wild: experimental test of eco-evolutionary dynamics. *Ecol. Lett.* **14**, 1084–1092 (2011).
15. Lawrence, D. et al. Species interactions alter evolutionary responses to a novel environment. *PLoS Biol.* **10**, e1001330 (2012).
16. Celiker, H. & Gore, J. Clustering in community structure across replicate ecosystems following a long-term bacterial evolution experiment. *Nat. Commun.* **5**, 4643 (2014).
17. Andrade-Domínguez, A. et al. Eco-evolutionary feedbacks drive species interactions. *ISME J.* **8**, 1041–1054 (2014).
18. Reznick, D. Hard and soft selection revisited: how evolution by natural selection works in the real world. *J. Hered.* **107**, 3–14 (2016).
19. Matthews, B., Aebischer, T., Sullam, K. E., Lundsgaard-Hansen, B. & Seehausen, O. Experimental evidence of an eco-evolutionary feedback during adaptive divergence. *Curr. Biol.* **26**, 483–489 (2016).
20. Harcombe, W. R., Chacón, J. M., Adamowicz, E. M., Chubiz, L. M. & Marx, C. J. Evolution of bidirectional costly mutualism from byproduct consumption. *Proc. Natl Acad. Sci. USA* **115**, 12000–12004 (2018).
21. Preussger, D., Giri, S., Muhsal, L. K., Oña, L. & Kost, C. Reciprocal fitness feedbacks promote the evolution of mutualistic cooperation. *Curr. Biol.* https://doi.org/10.1016/j.cub.2020.06.100 (2020).

22. Adamowicz, E. M., Muza, M., Chacón, J. M. & Harcombe, W. R. Cross-feeding modulates the rate and mechanism of antibiotic resistance evolution in a model microbial community of *Escherichia coli* and *Salmonella enterica*. *PLoS Pathog.* **16**, e1008700 (2020).
23. Rodríguez-Verdugo, A. & Ackermann, M. Rapid evolution destabilizes species interactions in a fluctuating environment. *ISME J.* **15**, 450–460 (2021).
24. Barber, J. N. et al. The evolution of coexistence from competition in experimental co-cultures of *Escherichia coli* and *Saccharomyces cerevisiae*. *ISME J.* **15**, 746–761 (2021).
25. Hart, S. F. M., Chen, C.-C. & Shou, W. Pleiotropic mutations can rapidly evolve to directly benefit self and cooperative partner despite unfavorable conditions. *eLife* **10**, e57838 (2021).
26. Kokko, H. et al. Can evolution supply what ecology demands? *Trends Ecol. Evol.* **32**, 187–197 (2017).
27. Nuismer, S. *Introduction to Coevolutionary Theory* (Macmillan Learning, 2017).
28. Stoltzfus, A. & McCandlish, D. M. Mutational biases influence parallel adaptation. *Mol. Biol. Evol.* **34**, 2163–2172 (2017).
29. Payne, J. L. et al. Transition bias influences the evolution of antibiotic resistance in *Mycobacterium tuberculosis*. *PLoS Biol.* **17**, e3000265 (2019).
30. Storz, J. F. et al. The role of mutation bias in adaptive molecular evolution: insights from convergent changes in protein function. *Philos. Trans. R. Soc. Lond. B* **374**, 20180238 (2019).
31. Gomez, K., Bertram, J. & Masel, J. Mutation bias can shape adaptation in large asexual populations experiencing clonal interference. *Proc. Biol. Sci.* **287**, 20201503 (2020).
32. Venkataram, S., Monasky, R., Sikaroodi, S. H., Kryazhimskiy, S. & Kacar, B. Evolutionary stalling and a limit on the power of natural selection to improve a cellular module. *Proc. Natl Acad. Sci. USA* **117**, 18582–18590 (2020).
33. Hom, E. F. Y. & Murray, A. W. Niche engineering demonstrates a latent capacity for fungal–algal mutualism. *Science* **345**, 94–98 (2014).
34. Wolfe, B. E. & Dutton, R. J. Fermented foods as experimentally tractable microbial ecosystems. *Cell* **161**, 49–55 (2015).
35. Chacón, J. M., Hammarlund, S. P., Martinson, J. N. V., Smith, L. B. & Harcombe, W. R. The ecology and evolution of model microbial mutualisms. *Annu. Rev. Ecol. Evol. Syst.* **52**, 363–384 (2021).
36. Blasche, S., Kim, Y., Oliveira, A. P. & Patil, K. R. Model microbial communities for ecosystems biology. *Curr. Opin. Syst. Biol.* **6**, 51–57 (2017).
37. Levy, S. F. et al. Quantitative evolutionary dynamics using high-resolution lineage tracking. *Nature* **519**, 181–186 (2015).
38. Venkataram, S. et al. Development of a comprehensive genotype-to-fitness map of adaptation-driving mutations in yeast. *Cell* **166**, 1585–1596.e22 (2016).
39. Jones, E. I., Bronstein, J. L. & Ferrière, R. The fundamental role of competition in the ecology and evolution of mutualisms. *Ann. N. Y. Acad. Sci.* **1256**, 66–88 (2012).
40. Boyer, S., Hérissant, L. & Sherlock, G. Adaptation is influenced by the complexity of environmental change during evolution in a dynamic environment. *PLoS Genet.* **17**, e1009314 (2021).
41. Blundell, J. R. et al. The dynamics of adaptive genetic diversity during the early stages of clonal evolution. *Nat. Ecol. Evol.* **3**, 293–301 (2019).
42. Good, B. H., Rouzine, I. M., Balick, D. J., Hallatschek, O. & Desai, M. M. Distribution of fixed beneficial mutations and the rate of adaptation in asexual populations. *Proc. Natl Acad. Sci. USA* **109**, 4950–4955 (2012).
43. Good, B. H., Martis, S. & Hallatschek, O. Adaptation limits ecological diversification and promotes ecological tinkering during the competition for substitutable resources. *Proc. Natl Acad. Sci. USA* **115**, E10407–E10416 (2018).
44. Zhu, Y. O., Siegal, M. L., Hall, D. W. & Petrov, D. A. Precise estimates of mutation rate and spectrum in yeast. *Proc. Natl Acad. Sci. USA* **111**, E2310–E2318 (2014).
45. Dunham, M. J. et al. Characteristic genome rearrangements in experimental evolution of *Saccharomyces cerevisiae*. *Proc. Natl Acad. Sci. USA* **99**, 16144–16149 (2002).
46. Yona, A. H. et al. Chromosomal duplication is a transient evolutionary solution to stress. *Proc. Natl Acad. Sci. USA* **109**, 21010–21015 (2012).
47. Sunshine, A. B. et al. The fitness consequences of aneuploidy are driven by condition-dependent gene effects. *PLoS Biol.* **13**, e1002155 (2015).
48. Gerrish, P. J. & Lenski, R. E. The fate of competing beneficial mutations in an asexual population. *Genetica* **102-103**, 127–144 (1998).
49. Desai, M. M. & Fisher, D. S. Beneficial mutation–selection balance and the effect of linkage on positive selection. *Genetics* **176**, 1759–1798 (2007).
50. Schiffels, S., Szöllosi, G. J., Mustonen, V. & Lässig, M. Emergent neutrality in adaptive asexual evolution. *Genetics* **189**, 1361–1375 (2011).
51. Nguyen, Ba,A. N. et al. High-resolution lineage tracking reveals travelling wave of adaptation in laboratory yeast. *Nature* **575**, 494–499 (2019).
52. Foster, K. R., Shaulsky, G., Strassmann, J. E., Queller, D. C. & Thompson, C. R. L. Pleiotropy as a mechanism to stabilize cooperation. *Nature* **431**, 693–696 (2004).
53. Sachs, J. L., Mueller, U. G., Wilcox, T. P. & Bull, J. J. The evolution of cooperation. *Q. Rev. Biol.* **79**, 135–160 (2004).
54. Harcombe, W. Novel cooperation experimentally evolved between species. *Evolution* **64**, 2166–2172 (2010).
55. Vasi, F., Travisano, M. & Lenski, R. E. Long-term experimental evolution in *Escherichia coli*. II. Changes in life-history traits during adaptation to a seasonal environment. *Am. Nat.* **144**, 432–456 (1994).
56. MacArthur, R. H. & Wilson, E. O. *The Theory of Island Biogeography* (Princeton Univ. Press, 2001).
57. Reznick, D., Bryant, M. J. & Bashey, F. *r*- and *K*-selection revisited: the role of population regulation in life-history evolution. *Ecology* **83**, 1509–1520 (2002).
58. Mueller, L. D. & Ayala, F. J. Trade-off between *r*-selection and *K*-selection in *Drosophila* populations. *Proc. Natl Acad. Sci. USA* **78**, 1303–1305 (1981).
59. Novak, M., Pfeiffer, T., Lenski, R. E., Sauer, U. & Bonhoeffer, S. Experimental tests for an evolutionary trade-off between growth rate and yield in *E. coli*. *Am. Nat.* **168**, 242–251 (2006).
60. Bachmann, H. et al. Availability of public goods shapes the evolution of competing metabolic strategies. *Proc. Natl Acad. Sci. USA* **110**, 14302–14307 (2013).
61. Lipson, D. A. The complex relationship between microbial growth rate and yield and its implications for ecosystem processes. *Front. Microbiol.* **6**, 615 (2015).
62. Orivel, J. et al. Trade-offs in an ant–plant–fungus mutualism. *Proc. Biol. Sci.* **284**, 20161679 (2017).
63. Fritts, R. K. et al. Enhanced nutrient uptake is sufficient to drive emergent cross-feeding between bacteria in a synthetic community. *ISME J.* **14**, 2816–2828 (2020).
64. Wortel, M. T., Noor, E., Ferris, M., Bruggeman, F. J. & Liebermeister, W. Metabolic enzyme cost explains variable trade-offs between microbial growth rate and yield. *PLoS Comput. Biol.* **14**, e1006010 (2018).

65. Cheng, C. et al. Laboratory evolution reveals a two-dimensional rate-yield tradeoff in microbial metabolism. *PLoS Comput. Biol.* **15**, e1007066 (2019).
66. Luckinbill, L. S. *r* and *K* selection in experimental populations of *Escherichia coli*. *Science* **202**, 1201–1203 (1978).
67. Oxman, E., Alon, U. & Dekel, E. Defined order of evolutionary adaptations: experimental evidence. *Evolution* **62**, 1547–1554 (2008).
68. Jasmin, J.-N., Dillon, M. M. & Zeyl, C. The yield of experimental yeast populations declines during selection. *Proc. Biol. Sci.* **279**, 4382–4388 (2012).
69. Laan, L., Koschwanez, J. H. & Murray, A. W. Evolutionary adaptation after crippling cell polarization follows reproducible trajectories. *eLife* **4**, e09638 (2015).
70. Blount, Z. D., Lenski, R. E. & Losos, J. B. Contingency and determinism in evolution: replaying life's tape. *Science* **362**, eaam5979 (2018).
71. Fukami, T. Historical contingency in community assembly: integrating niches, species pools, and priority effects. *Annu. Rev. Ecol. Evol. Syst.* **46**, 1–23 (2015).
72. Rainey, P. B. & Travisano, M. Adaptive radiation in a heterogeneous environment. *Nature* **394**, 69–72 (1998).
73. Meyer, J. R. et al. Repeatability and contingency in the evolution of a key innovation in phage lambda. *Science* **335**, 428–432 (2012).
74. Herron, M. D. & Doebeli, M. Parallel evolutionary dynamics of adaptive diversification in *Escherichia coli*. *PLoS Biol.* **11**, e1001490 (2013).
75. Hillesland, K. L. et al. Erosion of functional independence early in the evolution of a microbial mutualism. *Proc. Natl Acad. Sci. USA* **111**, 14822–14827 (2014).
76. Meroz, N., Tovi, N., Sorokin, Y. & Friedman, J. Community composition of microbial microcosms follows simple assembly rules at evolutionary timescales. *Nat. Commun.* **12**, 2891 (2021).
77. MacLean, R. C. The tragedy of the commons in microbial populations: insights from theoretical, comparative and experimental studies. *Heredity* **100**, 471–477 (2008).
78. Dunn, B. et al. Recurrent rearrangement during adaptive evolution in an interspecific yeast hybrid suggests a model for rapid introgression. *PLoS Genet.* **9**, e1003366 (2013).
79. Barillot, E., Lacroix, B. & Cohen, D. Theoretical analysis of library screening using a N-dimensional pooling strategy. *Nucleic Acids Res.* **19**, 6241–6247 (1991).
80. Baym, M., Shaket, L., Anzai, I. A., Adesina, O. & Barstow, B. Rapid construction of a whole-genome transposon insertion collection for *Shewanella oneidensis* by Knockout Sudoku. *Nat. Commun.* **7**, 13270 (2016).
81. Baym, M. et al. Inexpensive multiplexed library preparation for megabase-sized genomes. *PLoS ONE* **10**, e0128036 (2015).
82. Venkataram, S., Kuo, H., Hom, E., Kryazhimskiy, S. Early adaptation in a microbial community is dominated by mutualism-enhancing mutations. *Dryad* https://doi.org/10.6076/D14K5X (2022).

Acknowledgements

We thank G. Sherlock and K. Schwartz for providing the barcoded yeast library, S. Mayfield and F. Fields for laboratory equipment and help with algal husbandry, R. Dutton and M. Morin for help with sequencing, S. Rifkin and J. Bloom for help with microscopy, STARS students J. Yu and S. Rosemann for help with experiments, J. Meyer, A. Martsul and S. Sikaroodi for technical assistance, the Kryazhimskiy, Meyer and Hwa labs and D. Barrett, J. Borin, S. de Silva, S. Dunker, N. Garud, S. Harpole, C. Karakoç, H. Moeller, D. Petrov and P. Zee for feedback on the manuscript. Sequencing was done in part at the UCSD IGM Center (University of California, San Diego, La Jolla, CA). We acknowledge the San Diego Supercomputing Center for the use of the TSCC cluster for computing services. This project has been supported by the National Science Foundation CAREER grant 1846376 (E.F.Y.H.), Deutsches Zentrum für Integrative Biodiversitätsforschung (iDiv) grant DFG–FZT 118, 202548816 (E.F.Y.H.), BWF Career Award at the Scientific Interface grant 1010719.01 (S.K.), Alfred P. Sloan Foundation grant FG-2017-9227 (S.K.) and the Hellman Foundation (S.K.).

Author contributions

Conceptualization (S.V., E.F.Y.H. and S.K.), methodology (S.V., H.-Y.K. and S.K.), data acquisition (S.V.), analysis (S.V., H.-Y.K. and S.K.), initial manuscript (S.V. and S.K.), editing (S.V., H.-Y.K., E.F.Y.H. and S.K.), supervision (E.F.Y.H. and S.K.) and funding (S.K. and E.F.Y.H.).

Competing interests

The authors declare no competing interests.

Additional information

Extended data is available for this paper at https://doi.org/10.1038/s41559-022-01923-8.

Supplementary information The online version contains supplementary material available at https://doi.org/10.1038/s41559-022-01923-8.

Correspondence and requests for materials should be addressed to Sergey Kryazhimskiy.

Peer review information *Nature Ecology & Evolution* thanks Jeff Gore and the other, anonymous, reviewer(s) for their contribution to the peer review of this work. Peer reviewer reports are available.

https://doi.org/10.1038/s41559-022-01923-8

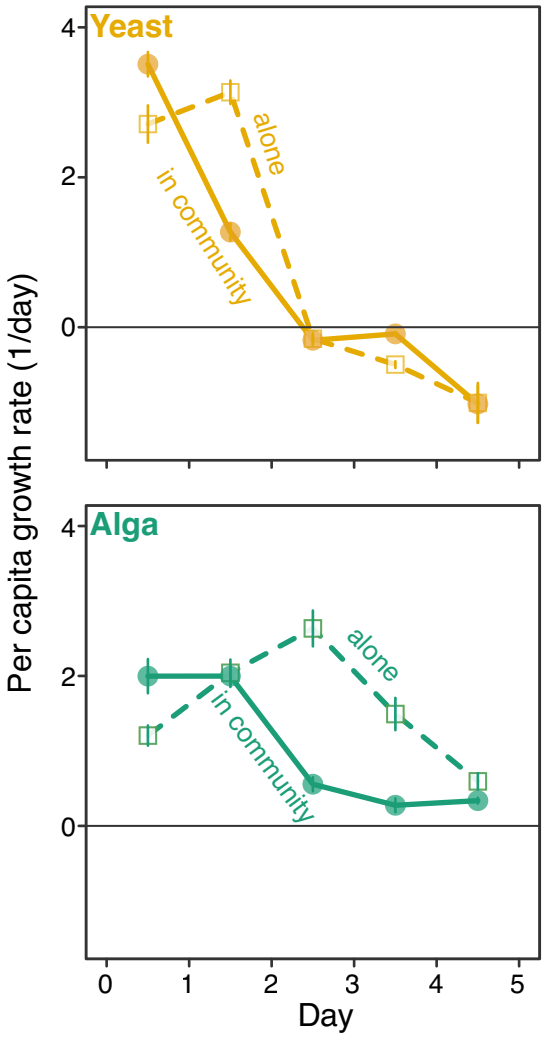

Extended Data Fig. 1 | Per capita net population change for the ancestral yeast and alga. Same data as in Fig. 1 ($n = 6$ except yeast alone where $n = 4$). Data points depict mean values ±1 SEM.

https://doi.org/10.1038/s41559-022-01923-8

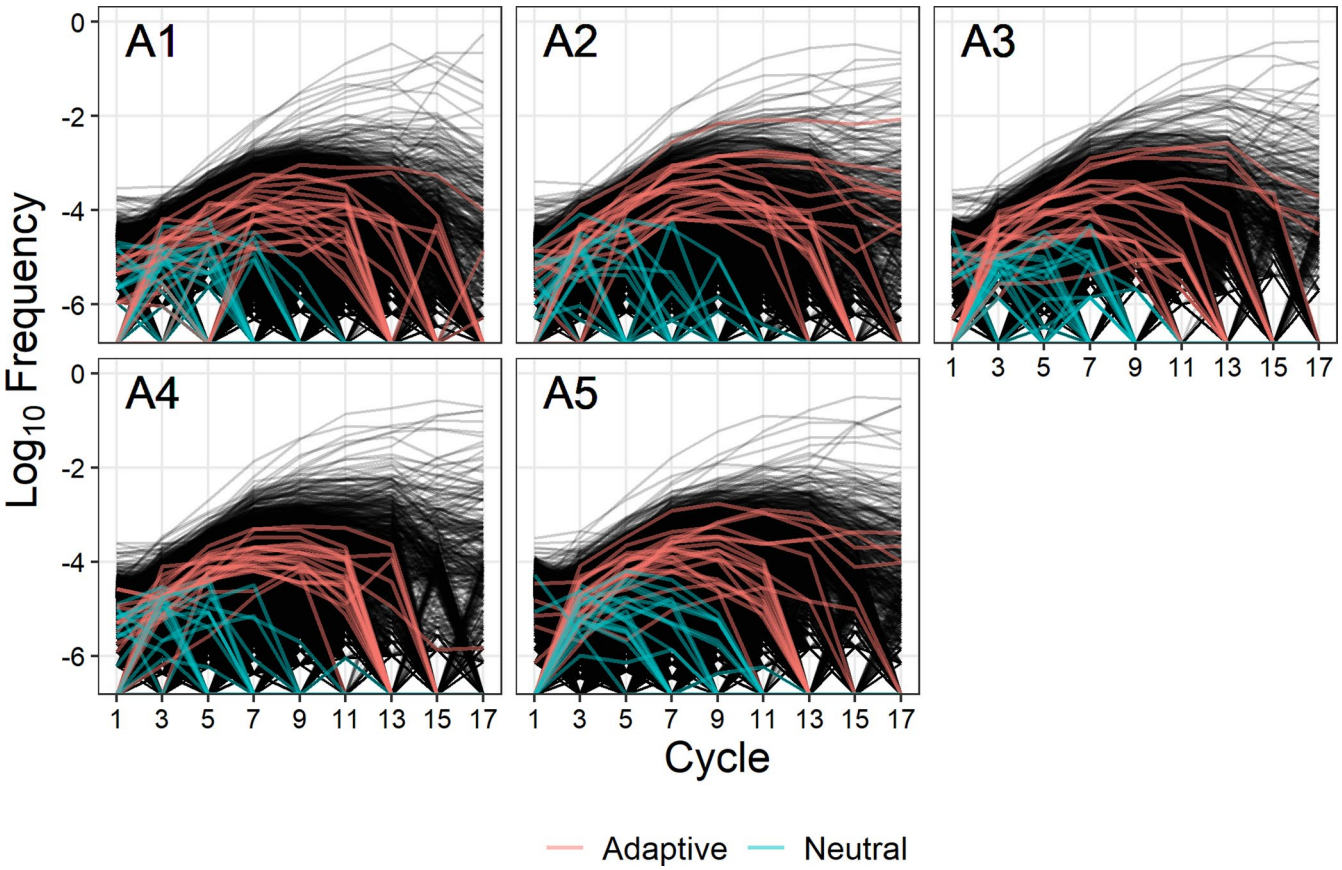

Extended Data Fig. 2 | Frequency trajectories of barcoded lineages in yeast in the A-condition. Each panel shows a BLT replicate population in the A-condition, as indicated. Lineage frequencies were measured at every odd cycle. Twenty random adapted lineages are shown in red, and twenty random neutral lineages are shown in blue.

https://doi.org/10.1038/s41559-022-01923-8

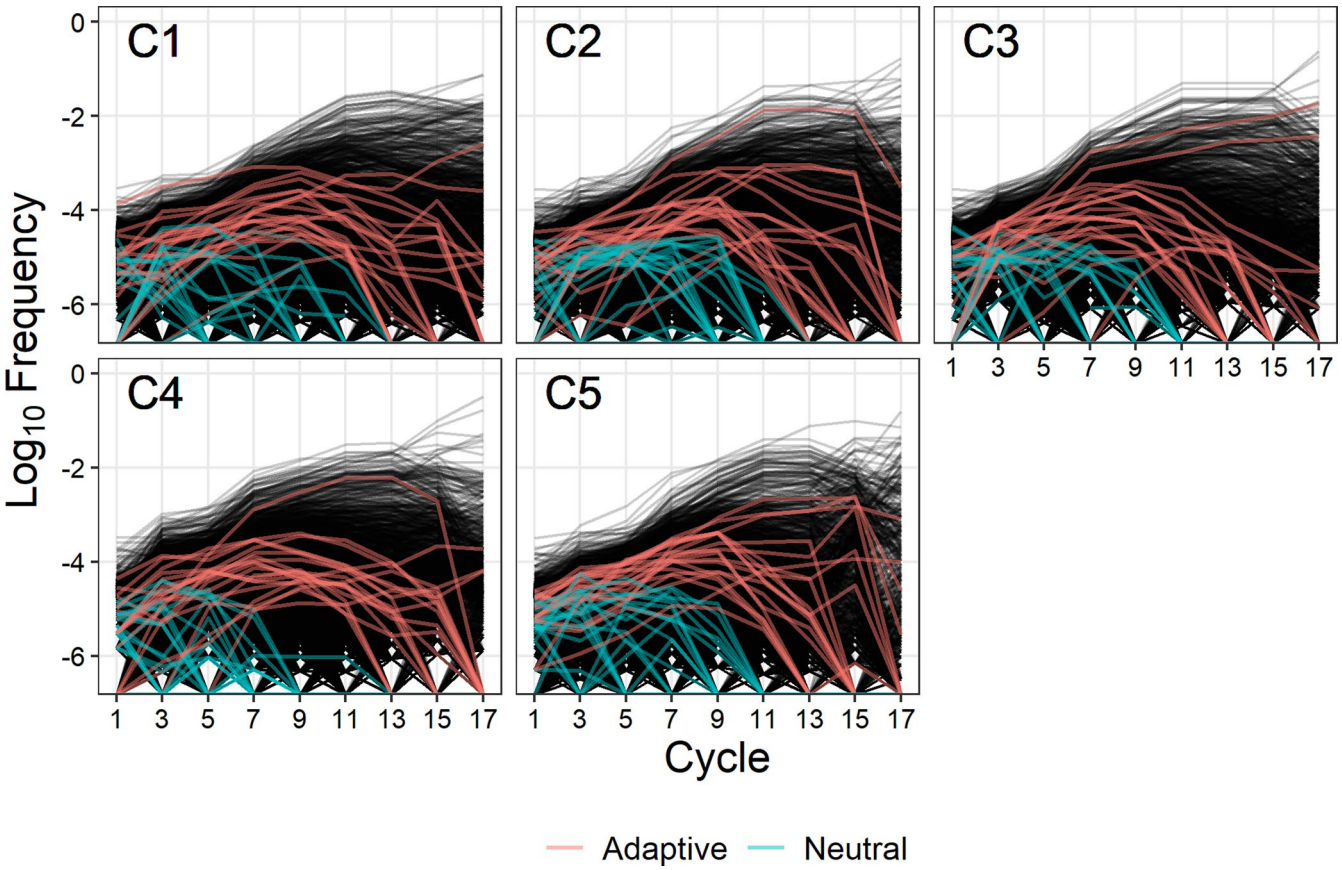

Extended Data Fig. 3 | Frequency trajectories of barcoded lineages in yeast in the C-condition. Each panel shows a BLT replicate population in the C-condition, as indicated. Lineage frequencies were measured at every odd cycle. Twenty random adapted lineages are shown in red, and twenty random neutral lineages are shown in blue.

https://doi.org/10.1038/s41559-022-01923-8

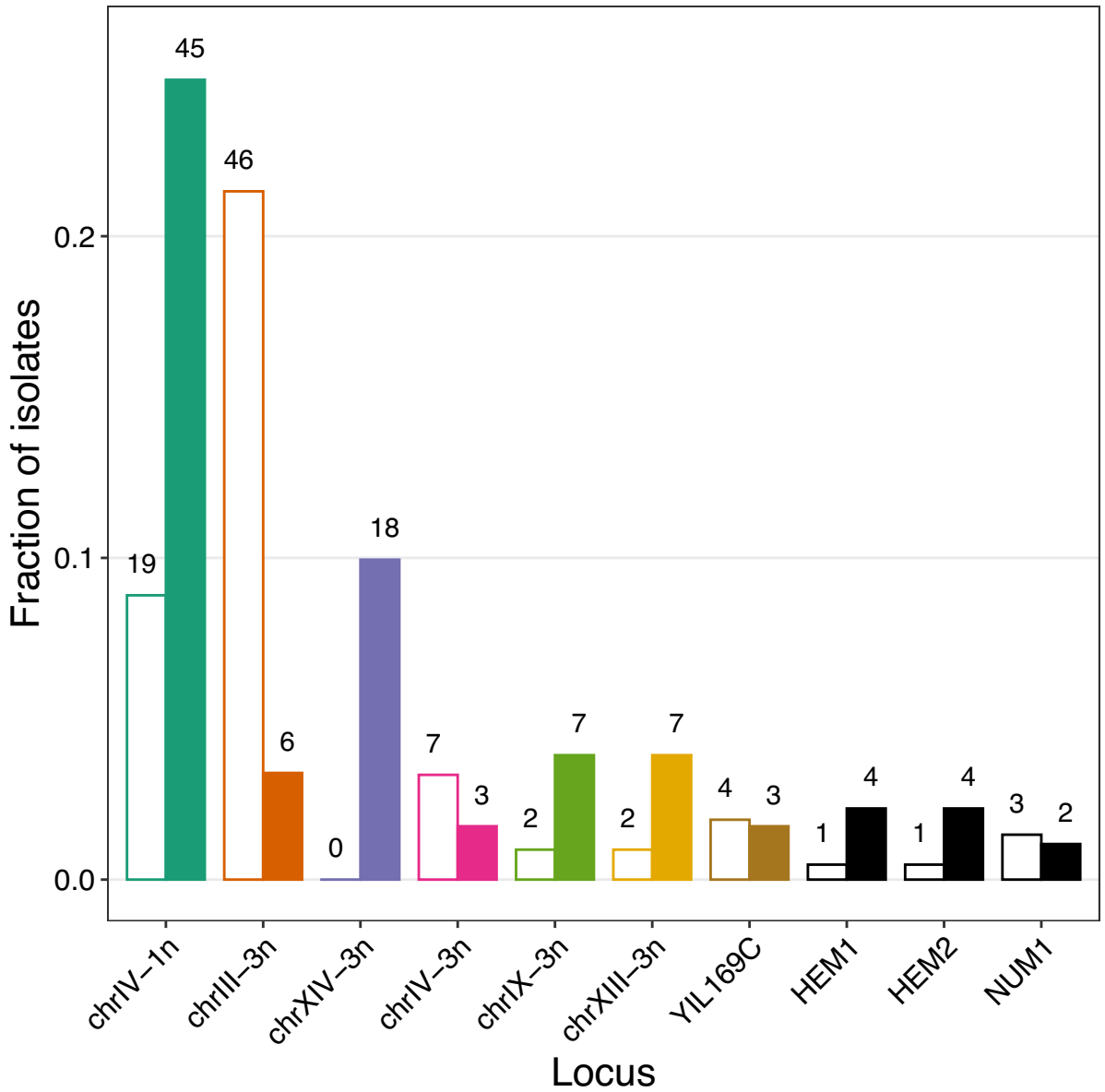

Extended Data Fig. 4 | Distribution of adaptive mutations across the most common driver loci. Driver loci with 5 or more mutations are shown. See Data S3 for the full distribution. Colors are the same as in Fig. 2.

https://doi.org/10.1038/s41559-022-01923-8

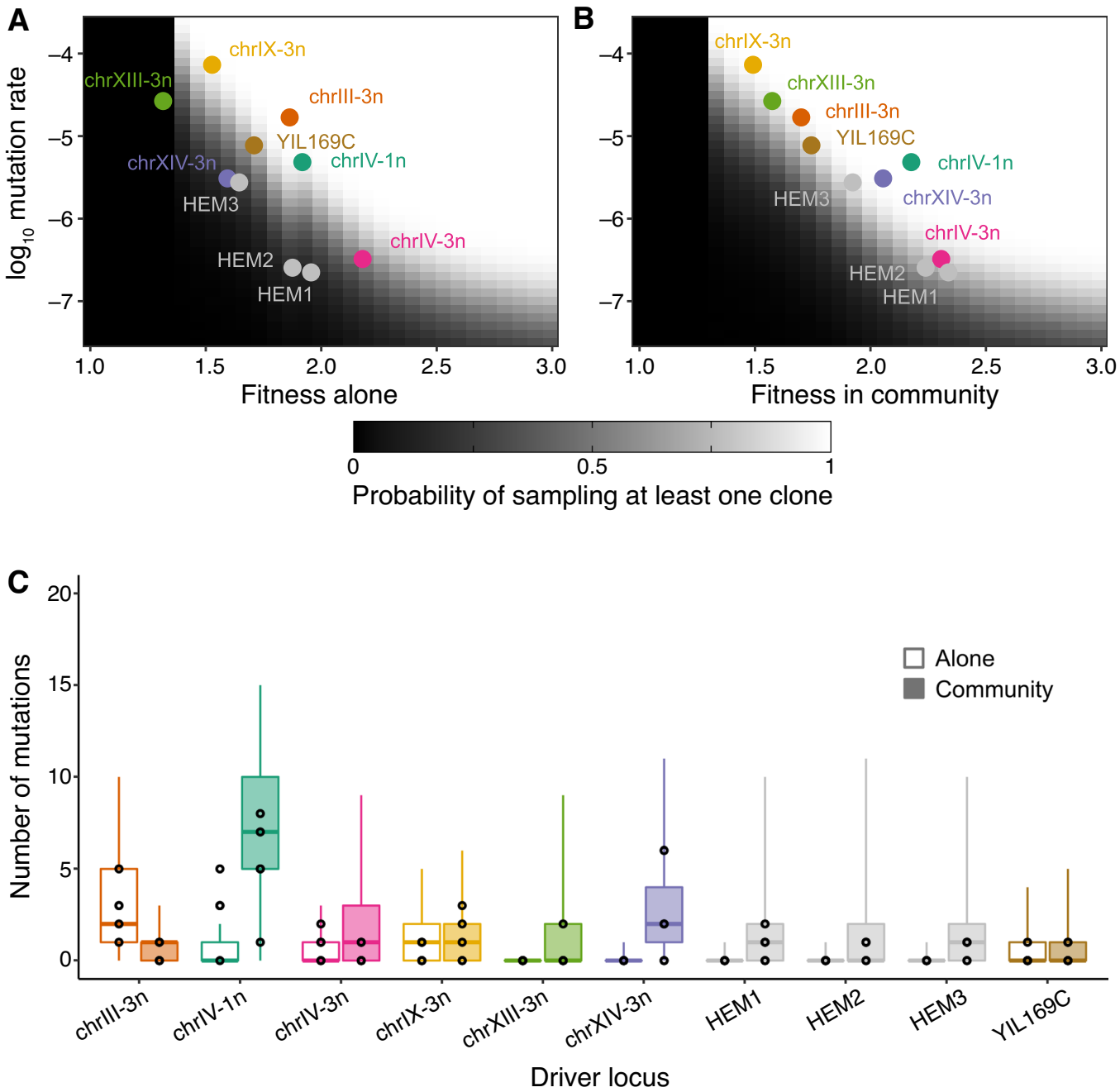

Extended Data Fig. 5 | Probabilities of observing adaptive mutations at the most common driver loci in the whole-genome sequencing data. A. Shades of gray represent the probability of sampling at least one clone with a beneficial mutation that arises at a certain rate (*y*-axis) and provides a certain fitness benefit in the A-condition (*x*-axis). The most common driver loci are shown by points (colors are the same as in Fig. 2). The estimated beneficial mutation rate and the selection coefficient for each mutation class are given in Table S3. **B**. Same as A but for the C-condition. The mutation rate for each locus is assumed to be the same in both conditions, but the selection coefficients vary. **C**. Black points show the number of sequenced clones with a given driver mutation found per replicate population in either A- (left) or C-condition (right; $n = 5$ replicate populations per condition). Box and whiskers show the distributions of these numbers found in our simulations (mid-line shows the median, boxes show the 25th and 75th quantiles, whiskers show the 5th and 95th quantiles).

https://doi.org/10.1038/s41559-022-01923-8

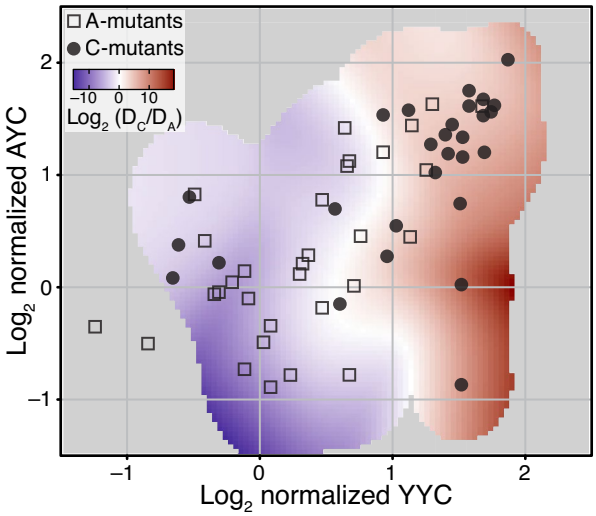

Extended Data Fig. 6 | Distribution of yields in mutant communities weighted by frequencies of adaptive mutations. The heatmap shows the ratio of estimated probability densities D_C and D_A of observing a given pair of yeast and alga yields in hypothetical communities formed by the alga ancestor and yeast mutants contending for fixation in the C- and A-conditions. Data points are identical to Fig. 3B in the main text. D_A and D_C are estimated by weighing each data point by the frequency of occurrence of the corresponding mutation among the sequenced A- and C-mutants, respectively (see Methods for details). Regions where either D_A or D_C falls below 0.03 are colored gray. YYC and YYA are normalized by the respective ancestral values.

https://doi.org/10.1038/s41559-022-01923-8

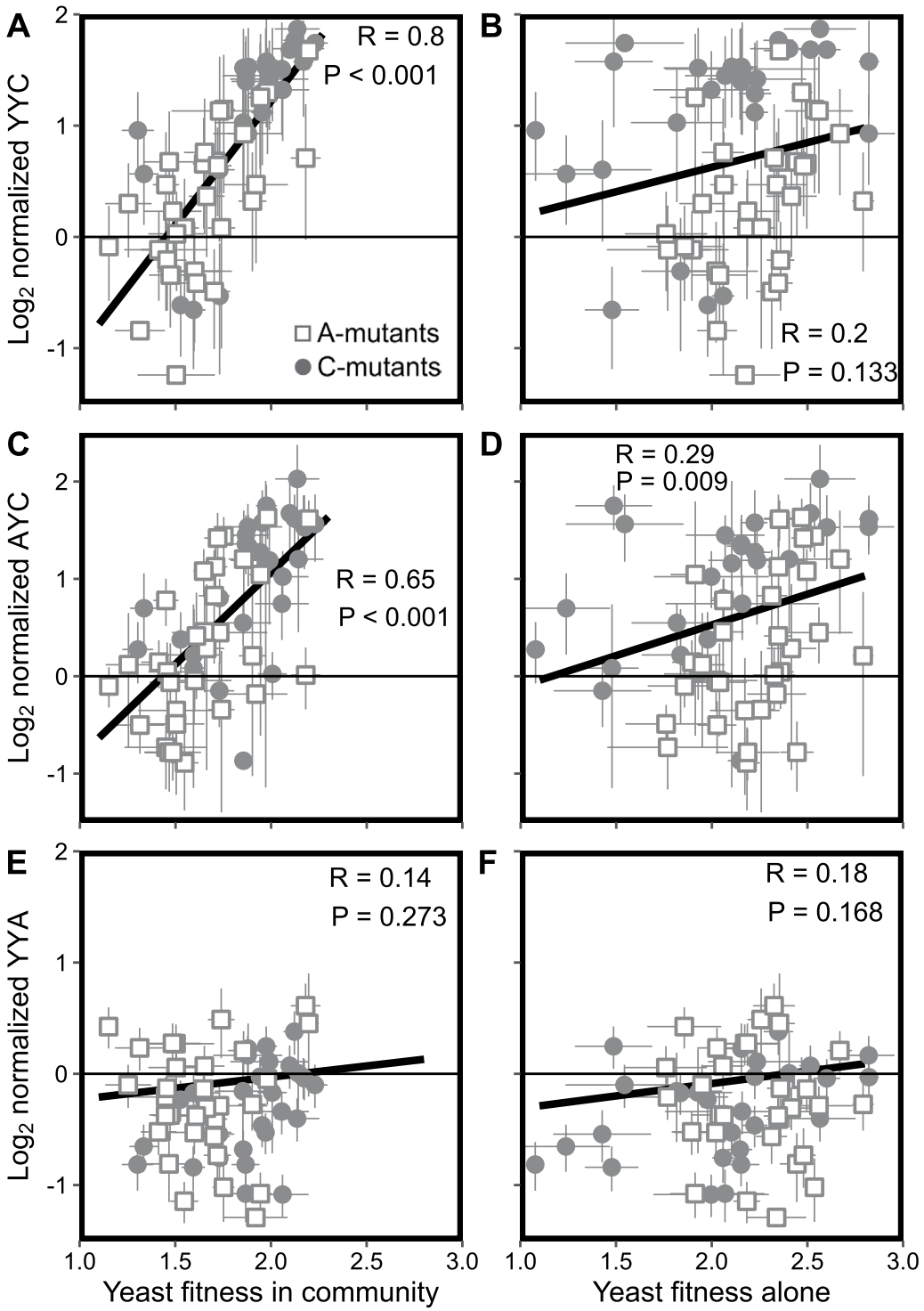

Extended Data Fig. 7 | Correlations between competitive fitness and yields. Normalization is relative to the ancestor. Error bars represent ±1 SEM. For all panels, $n = 31$ for A-mutants and $n = 28$ for C-mutants with three replicate fitness measurements and two replicate YYC, AYC and YYA measurements. Pearson correlation coefficients (R) are reported for each panel, as are P-values calculated by a two-tailed permutation test.

https://doi.org/10.1038/s41559-022-01923-8

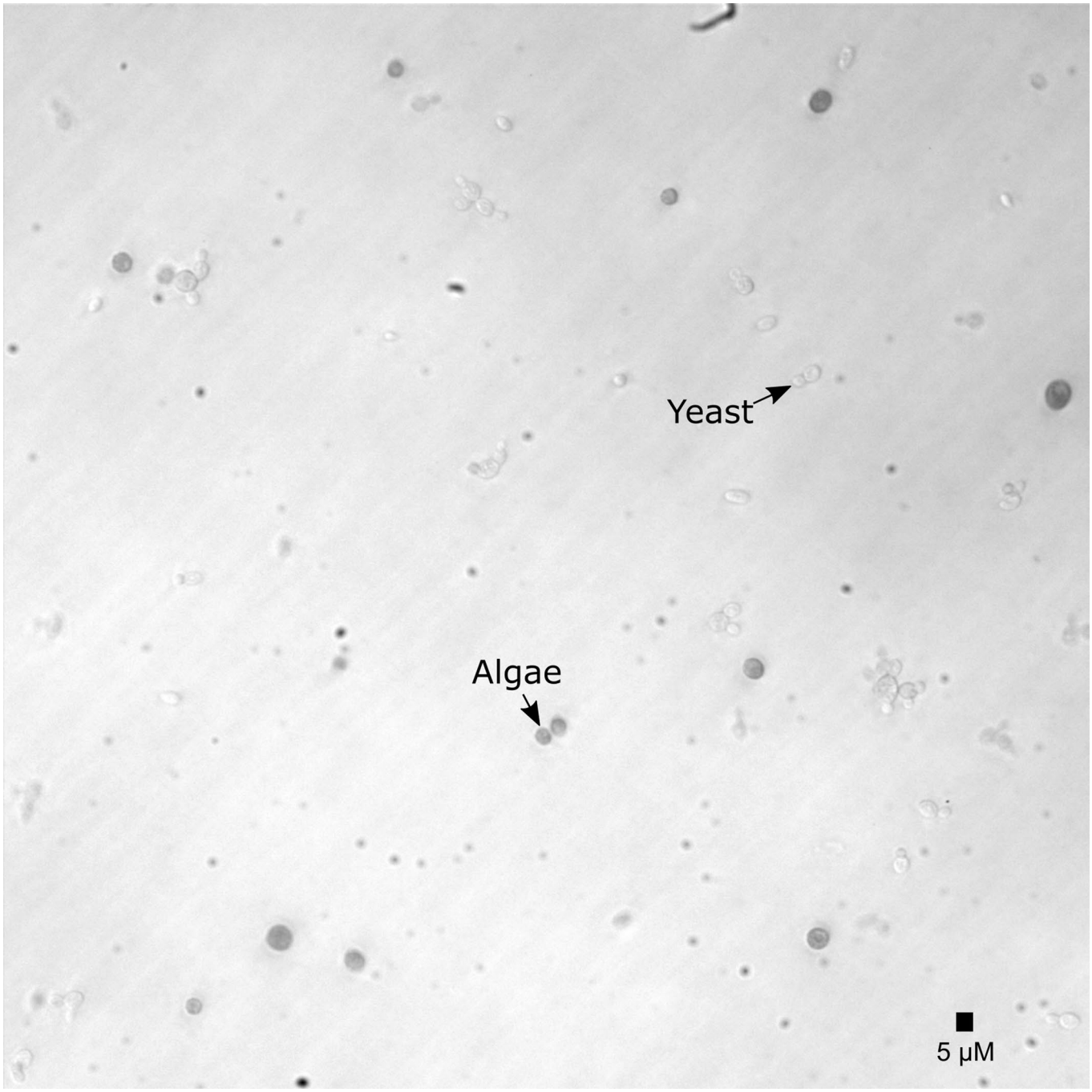

Extended Data Fig. 8 | Representative microscopy image showing lack of physical associations between yeast and algae cells. Mutant culture formed by the C-mutant C2 (barcode ID 109098) is shown. Yeast and alga cells are indicated with arrows. Similar observations were made for 17 other mutants (available on Dryad[82]).

https://doi.org/10.1038/s41559-022-01923-8

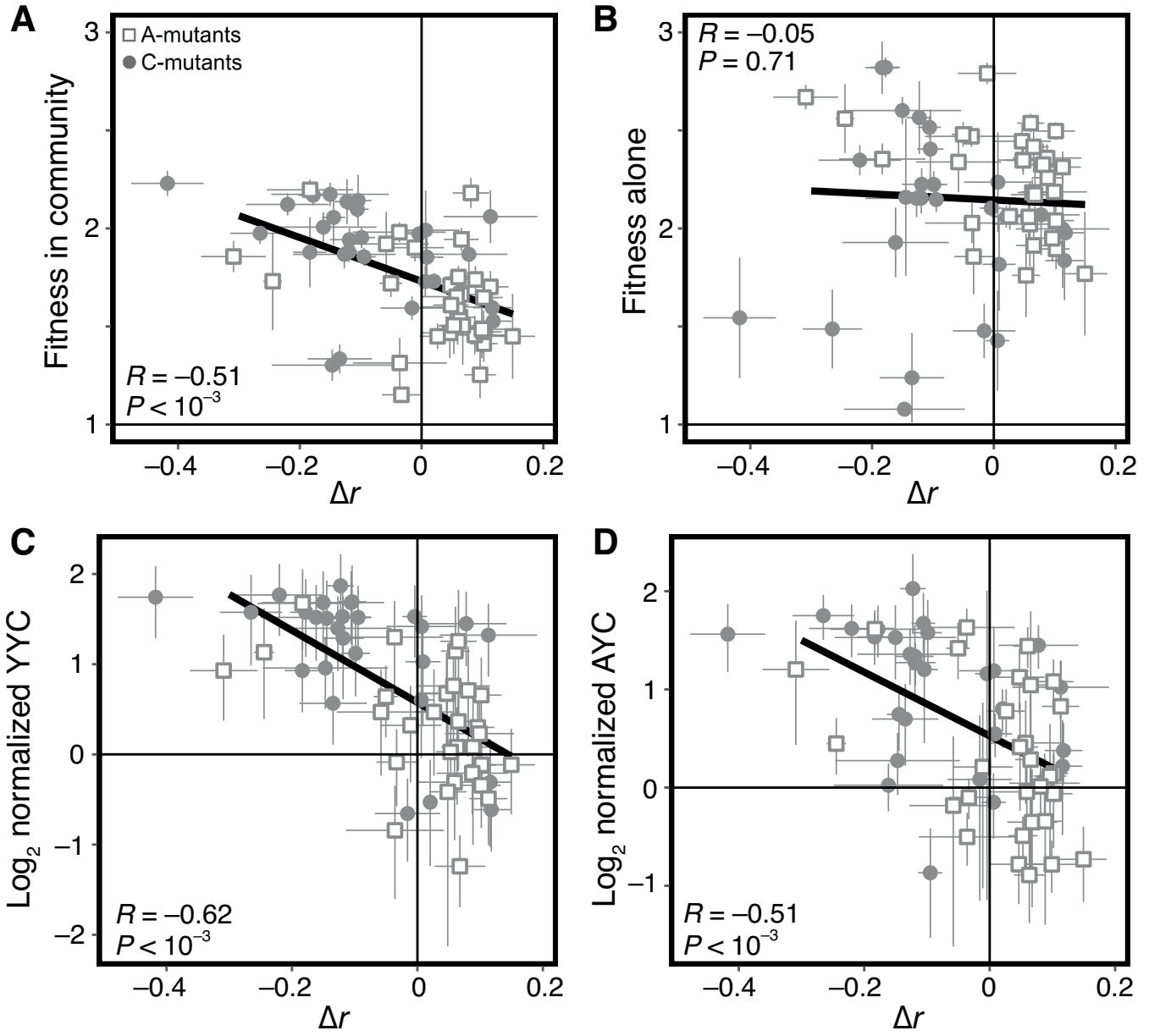

Extended Data Fig. 9 | Relationship between growth rate, yields and fitness. In all panels, normalization is relative to the ancestor. Error bars represent ±1 standard error of the mean. For all panels, n = 31 for A-mutants and *n* = 28 for C-mutants with three replicate fitness measurements and two replicate YYC, AYC and Δ*r* measurements. Pearson correlation coefficients (*R*) are reported for each panel, as are *P*-values calculated by a two-tailed permutation test.

https://doi.org/10.1038/s41559-022-01923-8

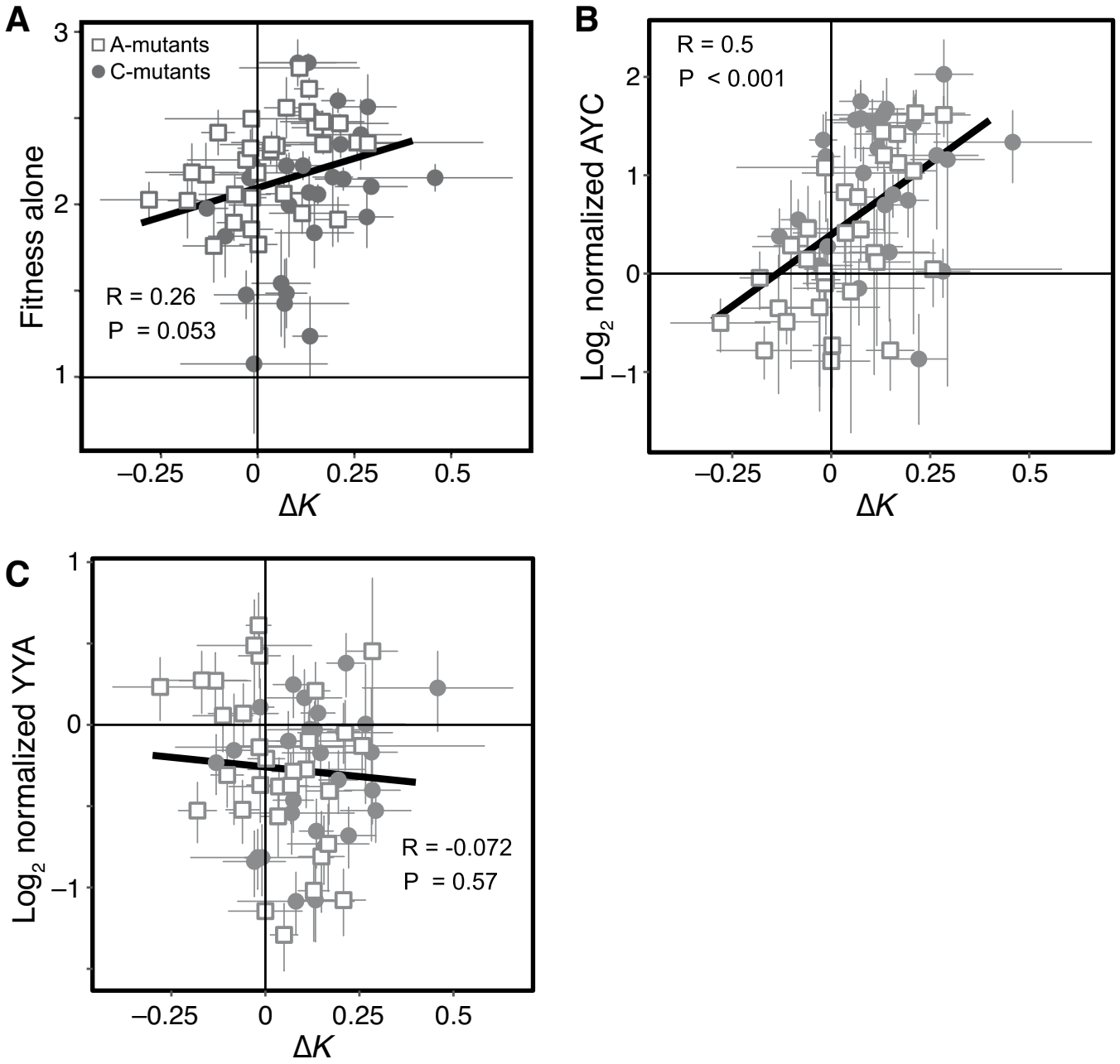

Extended Data Fig. 10 | Relationship between carrying capacity, yields and fitness. In all panels, normalization is relative to the ancestor. Error bars represent ±1 standard error of the mean. For all panels, $n = 31$ for A-mutants and $n = 28$ for C-mutants with three replicate fitness measurements and two replicate AYC, YYA and ΔK measurements. Pearson correlation coefficients (R) are reported for each panel, as are P-values calculated by a two-tailed permutation test.

nature portfolio

Corresponding author(s): Sergey Kryazhimskiy

Last updated by author(s): Sep 21, 2022

Reporting Summary

Nature Portfolio wishes to improve the reproducibility of the work that we publish. This form provides structure for consistency and transparency in reporting. For further information on Nature Portfolio policies, see our Editorial Policies and the Editorial Policy Checklist.

Statistics

For all statistical analyses, confirm that the following items are present in the figure legend, table legend, main text, or Methods section.

n/a	Confirmed	
☐	☒	The exact sample size (*n*) for each experimental group/condition, given as a discrete number and unit of measurement
☐	☒	A statement on whether measurements were taken from distinct samples or whether the same sample was measured repeatedly
☐	☒	The statistical test(s) used AND whether they are one- or two-sided *Only common tests should be described solely by name; describe more complex techniques in the Methods section.*
☐	☒	A description of all covariates tested
☐	☒	A description of any assumptions or corrections, such as tests of normality and adjustment for multiple comparisons
☐	☒	A full description of the statistical parameters including central tendency (e.g. means) or other basic estimates (e.g. regression coefficient) AND variation (e.g. standard deviation) or associated estimates of uncertainty (e.g. confidence intervals)
☐	☒	For null hypothesis testing, the test statistic (e.g. *F*, *t*, *r*) with confidence intervals, effect sizes, degrees of freedom and *P* value noted *Give P values as exact values whenever suitable.*
☐	☒	For Bayesian analysis, information on the choice of priors and Markov chain Monte Carlo settings
☐	☒	For hierarchical and complex designs, identification of the appropriate level for tests and full reporting of outcomes
☐	☒	Estimates of effect sizes (e.g. Cohen's *d*, Pearson's *r*), indicating how they were calculated

Our web collection on statistics for biologists contains articles on many of the points above.

Software and code

Policy information about availability of computer code

Data collection	Genome analysis was conducted using the following software packages: bowtie2 (v. 2.3.4.3), GATK (v. 4.0.11.0), ENSEMBL Variant Effect Predictor online tool (v. 100), Trimmomatic v. 0.36, DNAclust release 3, biopython v. 1.72, samtools v. 1.9, picardtools v. 2.18.15, bamtools v. 2.5.1, bcftools v. 1.9, bedtools v. 2.27.1, vcftools v. 0.1.16 and blast v. 2.7.1. DNA barcodes were counted using the software BarcodeCounter2, which was developed by author SV for this study (available at https://github.com/sandeepvenkataram/BarcodeCounter2).
Data analysis	Competitive fitness was estimated using the software fitness-assay-python, published in Venkataram et al Cell (2016) and available at https://github.com/barcoding-bfa/fitness-assay-python. The remaining analysis was conducted using custom software available on datadryad at https://doi.org/10.6076/D14K5X.

For manuscripts utilizing custom algorithms or software that are central to the research but not yet described in published literature, software must be made available to editors and reviewers. We strongly encourage code deposition in a community repository (e.g. GitHub). See the Nature Portfolio guidelines for submitting code & software for further information.

Data

Policy information about availability of data

All manuscripts must include a data availability statement. This statement should provide the following information, where applicable:

- Accession codes, unique identifiers, or web links for publicly available datasets
- A description of any restrictions on data availability
- For clinical datasets or third party data, please ensure that the statement adheres to our policy

All raw sequencing data is available on the US National Center for Biotechnology Information (NCBI) Sequence Read Archive (SRA) under BioProject PRJNA735257. All other raw data (e.g. growth data, variant calls, community yield etc) and analysis scripts can be found on Dryad at https://doi.org/10.6076/D14K5X.

Field-specific reporting

Please select the one below that is the best fit for your research. If you are not sure, read the appropriate sections before making your selection.

☒ Life sciences ☐ Behavioural & social sciences ☐ Ecological, evolutionary & environmental sciences

For a reference copy of the document with all sections, see nature.com/documents/nr-reporting-summary-flat.pdf

Life sciences study design

All studies must disclose on these points even when the disclosure is negative.

Sample size	Previous work (Levy et al 2015, Venkataram et al 2016) evolved 1-2 replicate populations and sampled ~200 adapted isolates for genotyping. These sample sizes were sufficient for statistical analysis. Consistent with these measurements, we conducted laboratory evolution of 5 replicate populations of each of two treatments, and isolated ~200 adaptive mutants from each treatment for genotyping and fitness measurement. For phenotypic measurement (e.g. yield) our facility had the capacity to grow 80 cultures in parallel in a single batch, and we thus selected 40 mutants from each treatment for these measurements.
Data exclusions	Some sequenced mutants had insufficient coverage for genotyping, and were thus excluded from further genomic analysis. Additional filters included removing mutants that were not adaptive, did not have valid fitness measurement data, or have fitness measurements that were too noisy. These mutants were thus excluded from all further analysis. As phenotyping commenced before these analyses were completed, 12 C-mutants and 9 A-mutants were excluded from our phenotypic analysis.
Replication	Evolution experiments were conducted with 5 replicates, and competitive fitness measurements were conducted with 3 replicate cultures for each treatment (alone and community). Phenotypic measurements were conducted with 2 replicate cultures for each measurement. Measurements of yeast mutants alone (YYA, growth rate, K) were repeated four times, as the initial set of two replicate measurements were poorly correlated ($R < 0.4$). Both of these initial replicates were discarded from all of our analyses.
Randomization	Randomization was not relevant for our study as both evolution treatments were instantiated with identical yeast populations (inoculated from the same pre-culture).
Blinding	Blinding was not relevant for our study as both yeast populations were initially identical. Furthermore, we had no a priori expectation in regards to the effect of algae on yeast evolution.

Reporting for specific materials, systems and methods

We require information from authors about some types of materials, experimental systems and methods used in many studies. Here, indicate whether each material, system or method listed is relevant to your study. If you are not sure if a list item applies to your research, read the appropriate section before selecting a response.

Materials & experimental systems

n/a	Involved in the study
☒	☐ Antibodies
☒	☐ Eukaryotic cell lines
☒	☐ Palaeontology and archaeology
☒	☐ Animals and other organisms
☒	☐ Human research participants
☒	☐ Clinical data
☒	☐ Dual use research of concern

Methods

n/a	Involved in the study
☒	☐ ChIP-seq
☒	☐ Flow cytometry
☒	☐ MRI-based neuroimaging